A Wind Tunnel Experiment for Trailing Edge Circulation Control on a 6% 2-D Airfoil up to Transonic Mach Numbers

Michael G. Alexander, Scott G. Anders, Stuart K. Johnson

NASA-Langley Research Center
Hampton, VA. 23681-001

ABSTRACT

A wind tunnel test was conducted on a six percent thick slightly cambered elliptical circulation control airfoil with both upper and lower surface blowing. Parametric evaluations of jet slot heights and Coanda surface shapes were conducted at mass flow coefficients (Cμ) from 0.0 to 0.12. The test data was acquired in the NASA Langley Transonic Dynamics Tunnel at Mach numbers of 0.8 and 0.3 at Reynolds numbers per foot of 1.05 x 10^6 and 2.43 x 10^5 respectively.

For the transonic condition, (Mach = 0.8 at α = +3°), it was generally found that the smaller slot and larger Coanda surface were more effective overall than other slot/Coanda surface combinations.

Generally it was found at Mach = 0.3 at α = +6° that the smaller slot and smaller Coanda surface were more effective overall than other slot/Coanda surface combinations.

INTRODUCTION

Circulation control is considered one of the most efficient methods for lift augmentation at low Mach numbers (ref. 1). The device augments an airfoil's lifting capability by tangentially ejecting a thin jet of high momentum air over a rounded trailing edge (ref. 2). The jet will remain attached to the surface as along as the low static pressures created by the jet are large enough to balance the centrifugal forces acting to detach the jet (ref. 3) (figure 1). The jet moves the separation point around the trailing edge toward the lower surface of the wing and entrains the external flow field. This entrainment and separation point movement produces a net increase in the circulation of the wing resulting in lift augmentation (ref 4.).
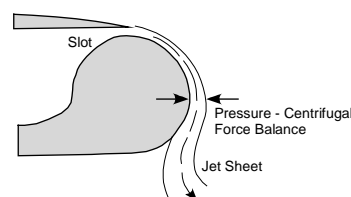

Figure 1 - Tangential Blowing Over a Coanda Surface

Numerous experimental circulation control tests using the Coanda effect to enhance lift have been conducted at subsonic velocities on relatively thick (15-percent) airfoil sections (ref. 5). The focus of this experiment is to evaluate the effectiveness of trailing edge circulation control on a thin airfoil section at transonic Mach numbers. A wind tunnel test was conducted on a six percent thick slightly cambered elliptical airfoil with both upper and lower surface slot blowing. Parametric evaluations of jet slot heights and Coanda surface shapes were conducted at mass flow coefficients (Cμ) from 0.0 to 0.12. The data was acquired in the NASA Langley Transonic Dynamics Tunnel at Mach = 0.8 at α = 3° and Mach= 0.3 at α = 6°, at a Reynolds number per foot of 1.05 x 10^6 and 2.43 x 10^5 respectively.

SYMBOLS

α	Angle-of-attack, degrees
Δ	Delta, incremental change
ρ	Density; (lbm/ft^3)
γ	Ratio of specific heat
A	Area (ft^2)
b	Model span (inch)
c	Chord (inch)
cref	Reference chord (30-inch)
CD	Discharge coefficient
C$_l$	Sectional lift coefficient

C_m	Sectional 0.25cref pitching moment coefficient
CP or C_p	Pressure coefficient
$C\mu$	Blowing coefficient
$\Delta Cl/C\mu$	Lift augmentation ratio
h	Average measured slot height (inch)
h/c	Non-dimensional slot height
$\dot{m}$	Mass flow (lbm/sec)
P_s	Free stream static pressure (psia)
P_0	Total pressure (psia)
q	Dynamic pressure (psi)
r	Radius
Rn/ft	Reynolds number per foot
t	Airfoil thickness
T_0	Total Temperature (R)
V	Velocity (ft/sec)
x	Chordwise distance (inch)
y	Span distance (inch)
y/b	Non-dimensional span location

Subscripts

jet	Air flow that exits nozzle
l	Lower
s	Slot
TE	Trailing edge
u	Upper

MODEL DESCRIPTION

The configuration tested in this experimental investigation is a semi-span rectangular circulation control airfoil with zero leading and trailing edge sweep having a circular end plate at the tip. The model as shown in figure 2a, was mounted in the wind tunnel on a splitter plate located approximately 3-ft off the tunnel wall.

Figure 2a - CCA Model – (view from right rear quarter, looking upstream)

The model incorporated circulation control by blowing tangentially from spanwise rectangular slots located upstream of a trailing edge "Coanda surface". The model has two separate and isolated internal plenums that fed air to either the upper or lower rectangular slot nozzle. The rectangular slot exits are located at x/cref = 0.9 and extends the full span (60-inches) of the model. The model is instrumented with a total of 157 static and total pressure taps, one accelerometer, and a type J thermocouple located in each plenum. The model has a surface finish of 32 μ-inch, and the Coanda surface external finish from upper slot exit to lower slot exit was of 16μ-inch.

Circulation Control Airfoil

The Circulation Control Airfoil (CCA) section is a simple six percent thick elliptical airfoil having 0.75-percent camber (figure 2b). The model span (b) was 60-inches with zero leading and trailing edge sweep. A reference chord (cref) of 30-inches gave the model an aspect ratio of two and a taper ratio of one. Common practice for testing semi-span models on a reflective plane is to refer to this as an aspect ratio four wing.
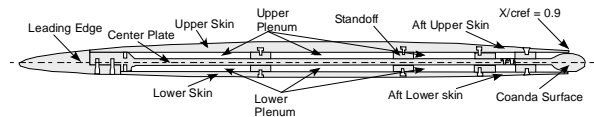

Figure 2b – CCA Airfoil Section

The CCA model tip is capable of accommodating either a 30-inch diameter circular end plate to promote 2-dimensional flow or a "t/2" tip used to evaluate 3-D effects. The model was tested with the end plate as shown in figure 2a.

Coanda Surface Definition

Three elliptical trailing edge surfaces (referred to as Coanda Surfaces) were manufactured with length-to-height ratios of 1.78:1, 2.38:1, and 2.98:1 as illustrated in Figure 3. The 2.38:1 Coanda surface installed on the CCA model with the end plate removed is shown in figure 4. The minor axis of the Coanda surface was aligned with the slot exit to ensure the minimum exit area occurred at x/cref = 0.9. The horizontal axis of the ellipse was then mapped to the camber line of the elliptical airfoil that formed a five-degree converging nozzle at the slot exit. The Coanda surface spanned the trailing edge of the model (60-inches).
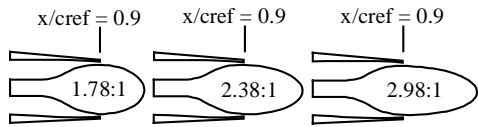
Figure 3 - Coanda Surfaces

Figure 4 - End View of a Coanda Surface and Aft Surfaces

Reference 6 provided guidelines for Coanda surface radius of curvatures as listed in table 1. It is not possible to meet the entire guideline radius of curvatures on a six percent thick airfoil. It was therefore decided that preference would be given to the slot radius of curvature in an effort to achieve initial jet attachment. As a result, a family of elliptical Coanda surfaces was chosen which have large slot radii of curvature and small trailing edge radii of curvature.

	Coanda		
	1.78 : 1	**2.38 : 1**	**2.98 : 1**
Chord (in)	27.82	28.09	28.36
r_s (in)	1.44	2.57	4.02
r_{TE} (in)	0.25	0.19	0.15
r_s/c	0.052	0.091	0.142
r_{TE}/c	0.009	0.007	0.005
Guidelines: r/c	0.02 to 0.06		
$h1/r_s$	0.024	0.014	0.009
$h2/r_s$	0.039	0.022	0.014
$h3/r_s$	0.051	0.028	0.018
$h1/r_{TE}$	0.14	0.18	0.23
$h2/r_{TE}$	0.22	0.30	0.37
$h3/r_{TE}$	0.29	0.38	0.48
Guidelines: h/r	0.01 to 0.08		

Table 1 – Coanda Radius and Slot Height Dimensions

Slot Definitions

Three upper and lower slot heights for each Coanda surface were possible for this wind tunnel investigation. The slot heights are given in table 2. A fourth slot height (h4) was constructed during the test using the upper surface small slot (h/c = 0.0012) aft skin by applying 4-layers of 0.0014-inch thick tape (0.0035-inches thick). The aft upper and lower removable surfaces were designed to set the slot heights by varying the internal mold line while not disturbing the outer mold line of the model. Average measured slot height (h) and chord lengths were used to determine the height to chord ratio (h/c) of each slot. Table 2 below lists the measured height and chords and the resulting h/c. Slot height to Coanda radius information is shown in table 1.

Slot	c (inches)	h (inches)	h/c
h1	27.82	0.035	0.0012
h2	28.09	0.056	0.0020
h3	28.36	0.073	0.0026
h4	28.36	0.0021	0.0007

Table 2 - Slot and Chord Measurements

Aft Surface

Three sets of aft surfaces were manufactured and attached to the main airfoil body which formed the upper and lower external airfoil contour as well as the internal five-degree convergent nozzle contour (figure 5).
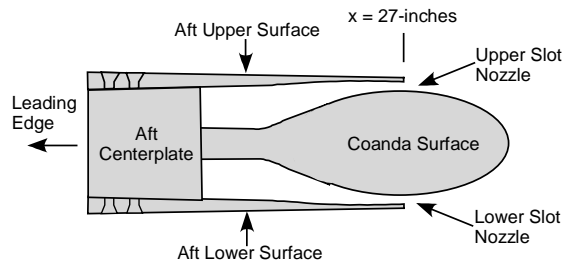

Figure 5 - Aft Surface Identification

The aft skins also contained chordwise surface static pressure taps at y/b = 0.5. Any aft surface in combination with any Coanda surface ensured the minimum nozzle area was located at the nozzle exit. Each aft surface also established a discrete slot height above the Coanda surface.

End Plate

The CCA model used a circular end plate to promote 2-D flow conditions. The end plate was

a 30-inch diameter circular plate constructed from a 0.25-inch thick aluminum plate with the outside edge beveled. The design of the end plate was based on sizing criteria found in reference 7. A removable cutout located at its trailing edge allowed for Coanda surface removal and replacement.

Internal Plenum

As seen in figure 2b, the airfoil section is divided into contiguous, separate, and isolated upper and lower plenums. The ratio of the slot height to plenum height ranged from 3.8 to 12.8 depending on the slot height. This ensured low flow velocities in the plenum that helped maintain uniform plenum flow.

Internal Plenum Screens

The model has the capability of holding six removable, 0.050-inch thick, high pressure-loss screens. The screens were fastened to the plenum floor and extended to the plenum ceiling. Each screen has a porosity of 30-percent and is capable of being placed in both upper and lower plenums at the three locations. The screen's porosity was sized using the method described in reference 8. It was determined through bench testing to use one screen in each plenum in the aft most position. The aft screen was located approximately x/cref = 0.72 and ran full spanwise and parallel to the slot nozzle.

Boundary Layer Trip

A boundary layer trip strip (ref. 9) was located 1.5-inches (measured along the surface) aft of the leading edge on the upper and lower surface. The trip strip used epoxy dots having a diameter of 0.038-inch, a thickness of 0.015-inch, and an edge-to-edge spacing distance between the epoxy dots of 0.098-inch.

INSTRUMENTATION

CCA Surface Static Pressures

A total of 83 external static surface pressure taps was located at y/b = 0.5 on the upper and lower airfoil surface (42 upper and 41 lower taps). There are two spanwise rows of 10-static pressures taps located at x/cref = 0.5 and 0.8 on each upper and lower airfoil surface.

Coanda Surface Static Pressures

Each Coanda surface had a total of 19-static surface pressure taps located at y/b = 0.5 every

10° radially from 0° to 180° with 0° and 180° at the nozzle exit (figure 6).
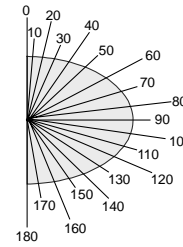
Figure 6 – Coanda Tap Placement

Total Pressures

Each plenum had six-total pressure taps. Their locations are given in table 3.

Taps	y/b	x/cref
1	0.2	0.3
2	0.2	0.8
3	0.45	0.8
4	0.5	0.8
5	0.55	0.8
6	0.8	0.8

Table 3 - Internal Plenum Tap Locations

Pressure taps at x/cref = 0.8 are located aft of the high loss screen and pressure taps x/cref = 0.3 are used to determine the total pressure entering the plenum from the intake nozzle. The total pressure for the plenum was averaged using taps 2, 3, 4, 5, and 6 to obtain the nozzle exit total pressure.

Thermocouples

The plenum has 2-iron-constantan, type J thermocouples located in each plenum to measure plenum total temperature.

FACILITY

This wind tunnel investigation was conducted in the NASA Langley Transonic Dynamics Tunnel (TDT) (ref. 10). The TDT is a closed circuit, continuous-flow, variable-pressure wind tunnel with a 16-foot square test section with cropped corners. The tunnel has the capability of using either air or R-134a gas as the test medium. The current investigation was conducted in air. The tunnel can operate up to Mach 1.2 and is capable of maximum Reynolds numbers of approximately three million per foot and dynamic pressures up to 2.29 psi in air.

Tunnel stagnation pressure can be varied from near vacuum to atmosphere.

Model Support

The TDT model support systems used for this test were a sidewall turntable and splitter plate as depicted in the figure 7. The splitter plate was located approximately 3-ft from the tunnel wall using wall standoffs. The rigid support and model instrumentation was placed inside an aerodynamic shape or "canoe" located between the splitter plate and the tunnel sidewall.
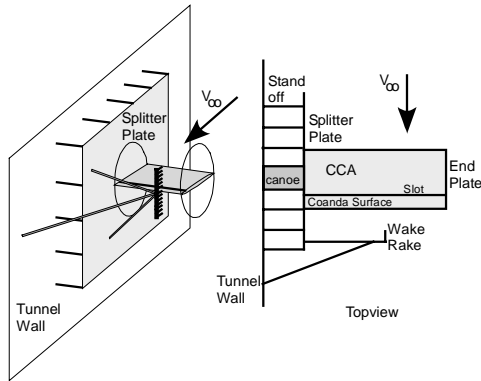

Figure 7 - CCA Model Installation in the TDT

Air Supply

Air was supplied to the test section via two 1-inch high-pressure flex lines delivering a maximum of 1-lbm/sec at 200-psia. Total temperature of the supply air was uncontrolled and ranged from –13°F to +70°F. Each supply line was attached to a control valve that regulated total pressure to the CCA model. A manually operated crossover line located upstream of the control valve allowed mass flow to be diverted from one line to another. After the control valve, each line of the supply air went through its dedicated critical flow venturi and then entered the model plenum.

TEST PROCEDURES AND CONDITIONS

Lift and Pitching Moment

The sectional lift coefficient (equation 1) and quarter chord pitching moment coefficient (equation 2) were obtained by numerically integrating (with the trapezoidal method) the local pressure coefficient at each $y/b = 0.5$ chordwise orifice from the upper and lower surface of the model.

$$C_l = \int_0^1 \left(C_{p_l} - C_{p_u} \right) d\left(x/c \right) * \cos\alpha \qquad (1)$$

$$C_{m.25} = \int_0^1 \left(C_{p_l} - C_{p_u} \right) \left(0.25 - \left(\frac{x}{c} \right) \right) d\left(\frac{x}{c} \right) \quad (2)$$

Mass Flow

The mass flow coefficient is calculated using equation 3.

$$C_\mu = \left(\frac{\dot{m} V_{jet}}{q_\infty S} \right) \qquad (3)$$

The ideal jet velocity (ft/s) was calculated (ref. 11) based on the assumption that the slot jet flow expands isentropically to the free-stream static pressure (equation 4).

$$V_{jet} = \sqrt{2 * R * T_o * g_c * \left(\frac{\gamma}{\gamma-1} \right) * \left[1 - \left(\frac{p_\infty}{P_{o_{plenum}}} \right)^{\frac{\gamma-1}{\gamma}} \right]} \qquad (4)$$

Mass flow was determined using equation 5 below. The discharge coefficient was obtained from critical flow venturi calibrations conducted in the NASA Jet Exit facility.

$$\dot{m} = CD * \left(A * V * \rho \right)_{throat} \qquad (5)$$

TEST CONDITIONS

The test conditions and ranges can be seen in table 4.

Mach	P_o(psia)	P_s (psia)	T_o (°F)	Rn/ft
0.3	2.7 - 4.1	2.6 - 3.8	67 - 94	3.6×10^5 - 5.5×10^5
0.8	3.0 - 4.1	2.0 - 2.7	95-125	7.8×10^5 - 1.0×10^6

Table 4 - CCA Test Range of Conditions

Data Corrections

No corrections were applied to account for tunnel flow angularity, wall interference effects, or end plate effects.

DISCUSSION OF RESULTS

Mach = 0.8; α = +3°

Coanda Surface Effect

In figures 8 and 9, Coanda surface effects are presented for the upper and lower slot blowing respectively. At Mach = 0.8 at α =3°,

each Coanda surface was capable of generating incremental lift and pitching moment at each blowing condition. Upper slot blowing generated positive lift and negative pitching moment increments while the lower slot blowing generated negative lift and positive pitching moment increments. Generally, the data in figure 8 displays three distinct regions. The first region is characterized by an increasing lift increment with increasing Cμ followed by a plateau region in most cases and then finally, a region of negative lift increment with further increasing Cμ. As the Coanda surfaces lengthened, increasing Cμ stretched the regions further. The Coanda surface effect observed in this data indicates the longer Coanda surface is more effective over the mid to high Cμ range, while all three Coanda surfaces are equivocal at the low end of Cμ. The data suggests the jet on the longer Coanda surface remains attached longer over a larger range of blowing coefficients while, conversely, the jet separates much sooner on the smaller Coanda surfaces. This data trend is generally followed in figure 9 for lower surface blowing. However, the lower surface blowing is not as effective in producing lift increment as the upper surface blowing over the same range of blowing coefficients. Also, as seen in figure 9, none of the Coanda surfaces tested were capable of generating incremental lift or pitching moment for h/c = 0.0026.

The lift augmentation ratio (ΔCl/Cμ) for upper and lower slot blowing is presented in figures 10 and 11 respectively. The upper and lower slot blowing data indicated the larger the Coanda surfaces, the greater the magnitudes of lift augmentation. It was observed that as Cμ increased, lift augmentation decreased in magnitude with the exception of the data obtained at h/c = 0.0026 (figure 11) which, as previously noted, generated insignificant lift increment. Maximum augmentation was typically achieved on each Coanda surface at mass flow coefficients less than 0.005. It appeared that the larger Coanda was more effective over a larger range of Cμ at any given h/c.

Slot Height Effect

In figures 12 and 13, slot height effects are presented for the upper and lower slot blowing. The data is the same data previously presented but replotted to better evaluate slot height effect. At Mach = 0.8 at α = +3°, the smallest slots were

most capable of generating incremental lift and pitching moment at each blowing condition.

The lift augmentation ratio for the upper surface slot blowing slot height effect is presented in figures 14 and 15. It is observed that the smaller the slot h/c on any given Coanda surface, the greater the lift augmentation. As stated earlier, as Cμ increased, the augmentation diminished.

Mach = 0.3 and α = +6°

Coanda Surface Effect

In figures 16 and 17, Coanda surface effects are presented for the upper and lower slot blowing respectively. At Mach = 0.3 at α = +6°, each Coanda surface was capable of generating incremental lift and pitching moment at each blowing condition. Increasing incremental lift and moments are observed with increasing blowing rate with upper slot blowing creating positive lift increments and negative pitching moment increments, while lower slot blowing created negative lift and positive pitching moment increments. Upper and lower slot blowing incremental lift and moment data trends for each Coanda surface displayed a marked decrease in effectiveness at higher blowing rates. Also observed is an apparent 'pinch down' in the h/c = 0.0012 and 0.0020 slot data from Cμ = 0.06 to 0.08 that diminished as the Coanda surface increased. This may indicate a reattachment effect (in the immediate region of the slot) followed by a lull where there is little flow turning with Cμ increment. The lull is then followed by a period of flow turning around the Coanda Bulb due to the increased Cμ. On the upper surface blowing (figure 16), as the slot size (h/c) was increased, the preferred Coanda went from 1.78:1 at h/c = 0.0012 to 2.98:1 at h/c = 0.0026. It is observed in figure 17, the lower slot blowing force and moment increments followed the same trend as the upper slot blowing, but had reduced absolute values of force and moment increments than that of the upper surface blowing (figure 16). Differences in upper and lower slot blowing are probably due to angle-of-attack, camber, and jet exit angle. At Mach = 0.3 at α = +6°, the smaller slot (h/c = 0.0012) on the smaller Coanda surface 1.78:1 generated the largest increments over the largest Cμ range, making it the preferred surface at this test condition.

The lift augmentation ratio for upper and lower slot blowing is presented in figures 18 and

19 respectively. As was seen in the M=0.8 data, the lift augmentation decreased with increasing Cμ. Unlike the M=0.8 data, the smallest Coanda generated the largest augmentation ratio from all of the data shown. However, the smallest Coanda did not achieve the largest augmentation ratio for all slot heights. At h/c=0.0012 the 1.78:1 Coanda surface achieves the largest augmentation ratio. At h/c=0.0026, the 2.98:1 Coanda surface achieves the largest augmentation ratio.

Slot Height Effect

In figures 20 and 21 slot effects are presented for the upper and lower slot blowing. The data is the same data previously presented but replotted to better evaluate slot height effect. For each Coanda surface the data suggests that the smaller the h/c, the greater ΔCl and ΔCm generated for the upper (figure 20) and lower slot blowing (figure 21).

The lift augmentation ratio for the upper and lower slot blowing is presented in figures 22 and 23. In figure 22, at each Coanda surface tested, the smaller the slot, the greater its augmentation ratio becomes.

Nozzle Pressure Ratio

In figure 24, incremental lift data are presented at Mach numbers of 0.8 and 0.3 as a function of Nozzle Pressure Ratio (NPR). The surface and slot height noted in the figure was the best configuration for each Mach number. The NPR data are presented as an aid in interpreting the data. For NPR's greater than 1.893 the exit slot is choked and therefore the jet is supersonic.

Velocity Ratio

In figure 25, incremental lift data are presented at Mach numbers of 0.8 and 0.3 as a function of velocity ratio for the same configurations used in the NPR figures. These data are presented for reference purposes similar to the NPR data to orient the reader to the ranges of velocity ratios tested.

Pressure Distributions

Figure 26a presents data taken at Mach = 0.8 at α = +3, for the (2.98:1) Coanda and h/c=0.0012 slot configuration. A Cμ effect was not observed on the leading edge of this airfoil. The data suggests a possible weakening of the upper surface shock with increasing Cμ. In figure 26b, which shows the Coanda surface

pressures, the pressure data suggested a shock just aft of the nozzle exit with flow re-attachment and pressure recovery. The surface pressure data indicated the shock moved aft with increasing Cμ. Also note at Cμ = 0.017 and 0.02, the jet completely detaches from the surface.

Figure 27a presents data taken at Mach = 0.3 at α = +6 for the 1.78:1 Coanda and h/c=0.0012 slot configuration. A Cμ effect is observed on the leading edge at this test condition. As Cμ was increased, the leading edge suction peak broadened further downstream up to a Cμ = 0.046. The data indicated at Cμ ≥ 0.046 that no further enhancement of the leading edge suction are observed. In figure 27b, which shows the Coanda bulb pressures, the pressure data at Cμ ≥ 0.046 suggested a shock just aft of the nozzle exit followed by flow re-attachment. As Cμ is increasing an increasing negative pressure field is seen over the remaining length of the Coanda bulb surface. In addition, the surface pressure data suggests that the shock may be moving aft with increasing Cμ.

CONCLUSIONS

A wind tunnel experiment at Mach numbers 0.3 and 0.8 on a 2-D, six percent thick airfoil with a modified trailing edge to enhance the Coanda effect by tangential jet slot blowing was accomplished. Incremental sectional lift and quarter chord pitching moment and lift augmentation ratio data were presented to support any indications of slot height and Coanda surface effects.

At the transonic cruise condition, Mach = 0.8 at α = +3°, it was found that the effectiveness increased with decreasing slot height and increasing Coanda surface elliptical ratio.

At the low speed condition, Mach =0.3 at α = +3°, it was found that the effectiveness increased with decreasing slot height and decreasing Coanda surface elliptical ratio.

REFERENCES

1) Novak, C.J.; Cornelius, K.C.; Road, R.K.: Experimental Investigations of Circular Wall Jet on a Circulation Control Airfoil. AIAA 87-0155.

2) Englar, R.J.: Investigations into and Application of the High Velocity Circulation Control Wall Jet for High Lift and Drag Generation on STOL Aircraft. AIAA 74-502.

3) Ahuja, K.K.; Sankar, L.N.; Englar, R.J.; Munro, S. Liu, Yi.: Application of Circulation Control Technology to Airframe Noise Reduction. GTRI Report: A5928/1, NASA Grant NAG-1-2146, February 15, 2000.

4) Abramson, J.: The Low Speed Characteristics of a 15-Percent Quasi-Elliptical Circulation Control Airfoil with Distributed Camber. David W. Taylor Naval Ship R&D Center Report DTNSRDC/ASED-79/07 (AD-A084-176), May 1979.

5) Nielsen, J. N.; and Bigger, J. C.: Recent Progress in Circulation Control Aerodynamics. AIAA Paper 87-0001, 1987.

6) Rogers, E.; and Abramson, J.: Selected Notes on Coanda Circulation Control Airfoils. unpublished notes, NSWC, 17 April 2002.

7) S.F. Hoerner; and H.V. Borst: Fluid-Dynamic Lift. 2nd edition (June 1992), ISBN: 9998831636.

8) Blevins, Robert, D.: Applied Fluid Dynamics Handbook. Van Nostrand Reinhold Company, New York, 1984.

9) Holmes, J. D.: Transition Trip Technique Study in the McAir Advanced Design Wind Tunnel. Technical Memorandum, May 1984.

10) Staff, Aeroelasticity Branch: *The Langley Transonic Dynamics Tunnel.* LWP-799 September 23, 1969.

11) Englar, Robert, J.: Two-Dimensional Transonic Wind Tunnel Test of Three 15-percent Thick Circulation Control Airfoils. Technical Note, AL-128, December 1970.

Slot (h/c = 0.0012)

Slot (h/c = 0.0020)

Slot (h/c = 0.0026)

Coanda Surface   Slot Height

1.78:1   h/c = 0.0012

2.38:1   h/c = 0.0020

2.98:1   h/c = 0.0026
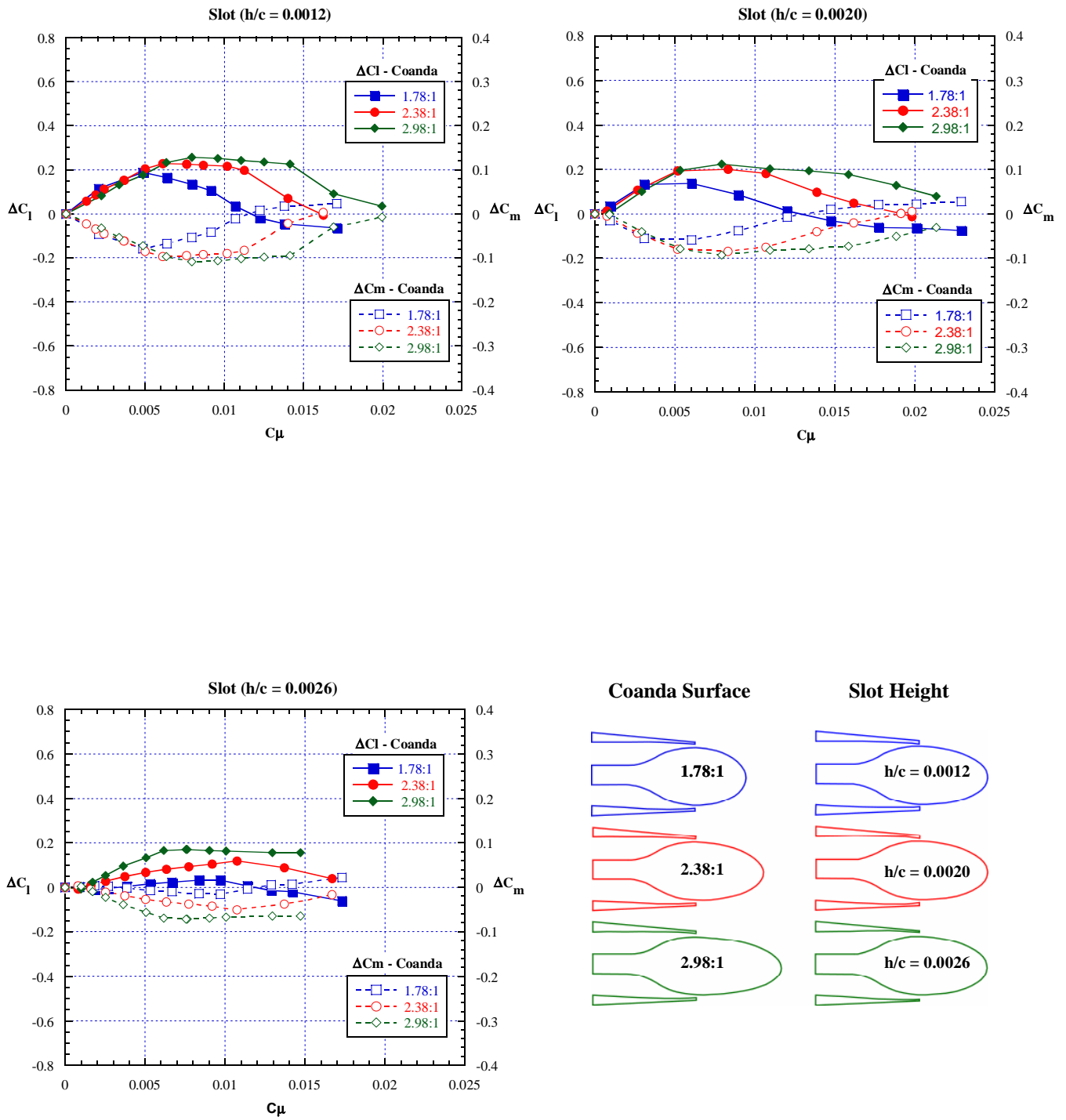
Figure 8 - Coanda surface effect, upper slot blowing, Mach = 0.8, α = +3°.

415
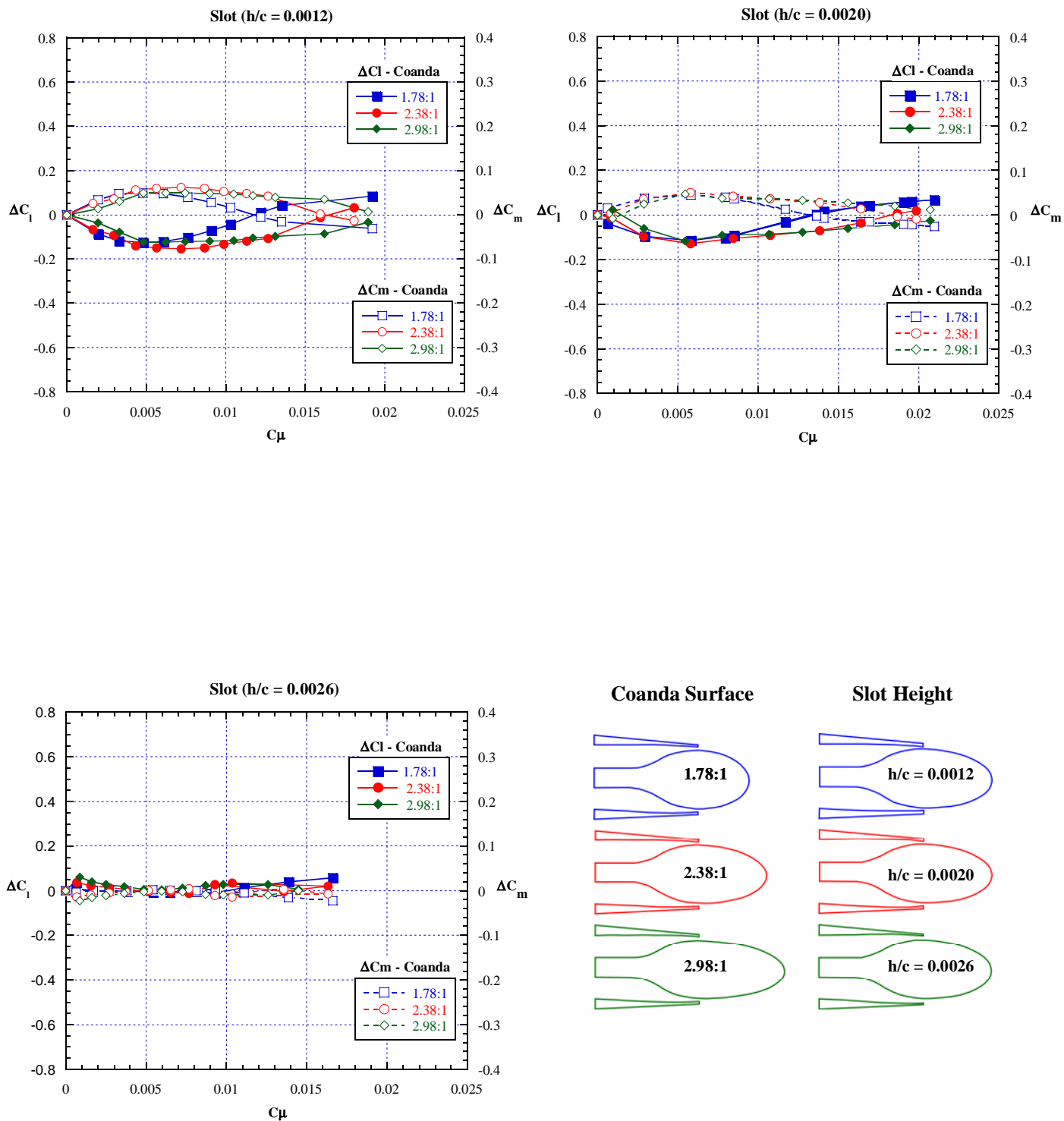
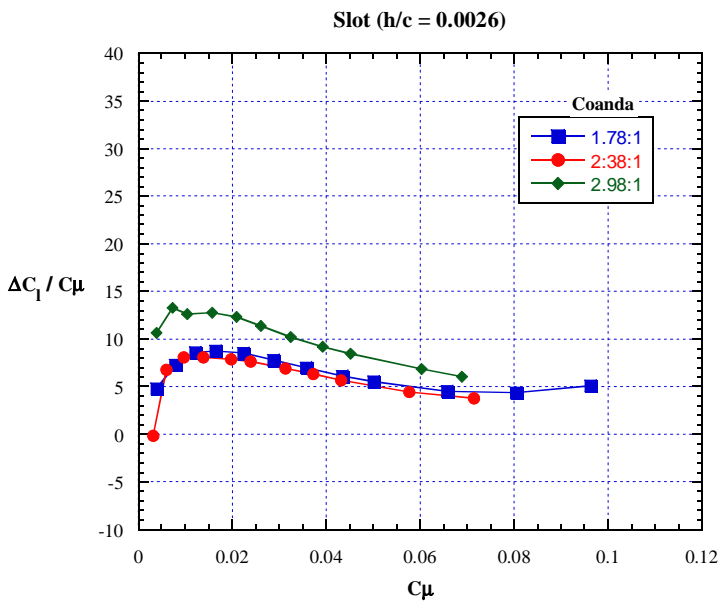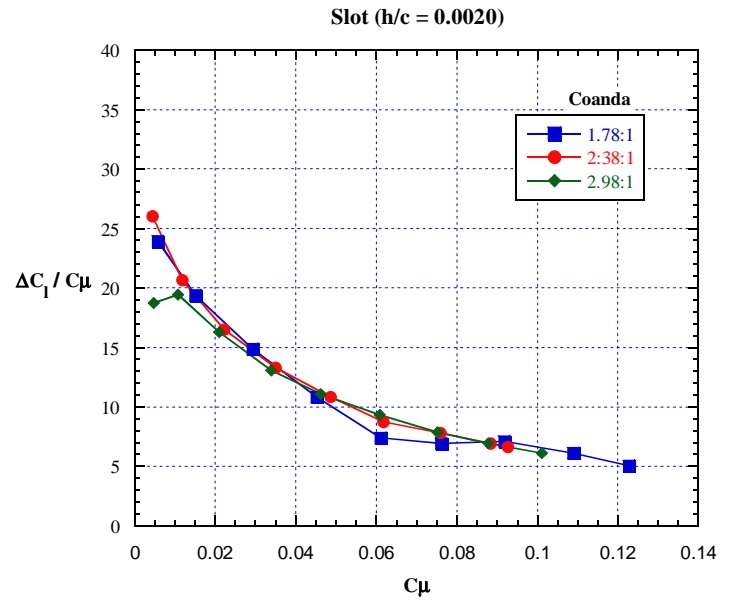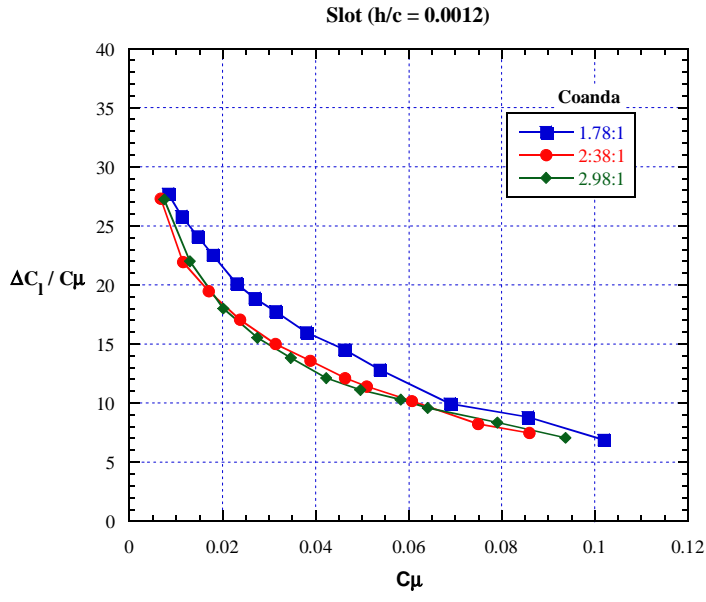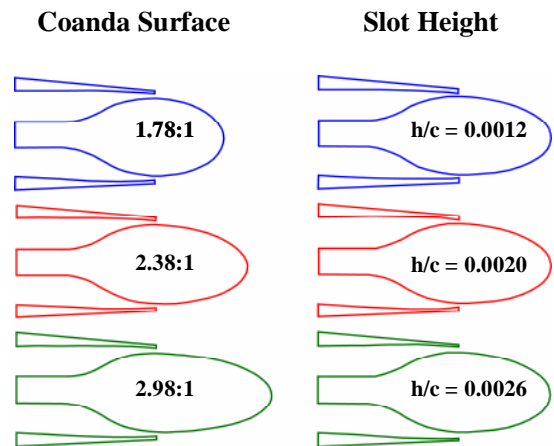Figure 9 - Coanda surface effect, lower slot blowing, Mach = 0.8, α = +3°.

Slot (h/c = 0.0012)

Slot (h/c = 0.0020)

Slot (h/c = 0.0026)

Coanda Surface
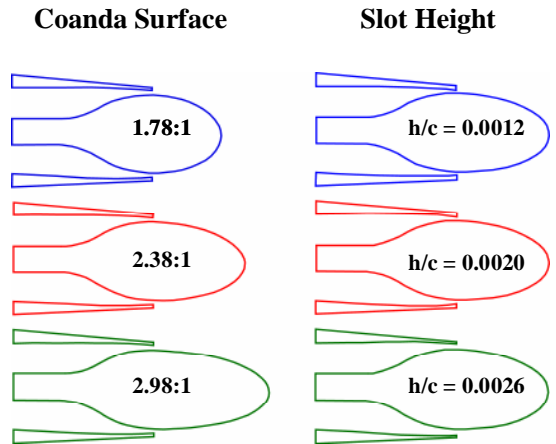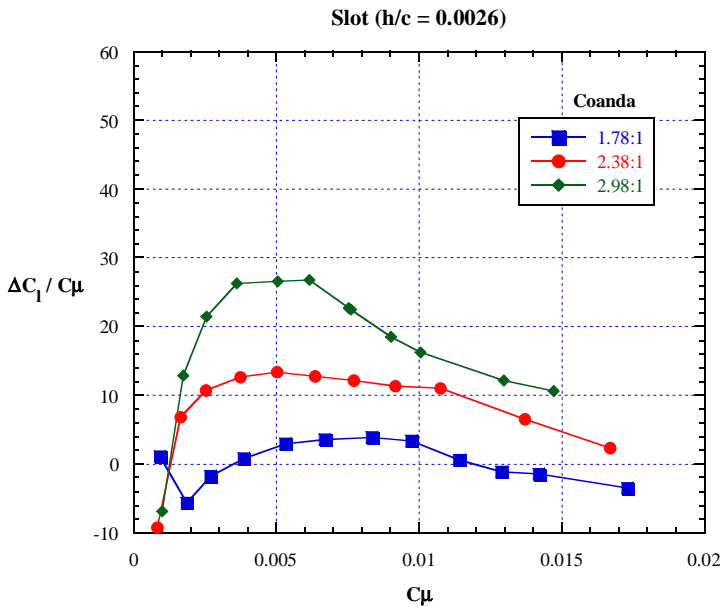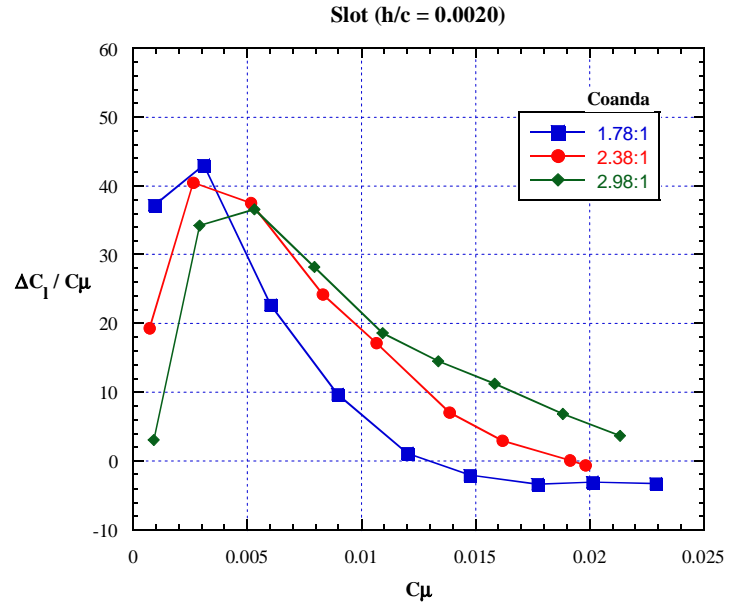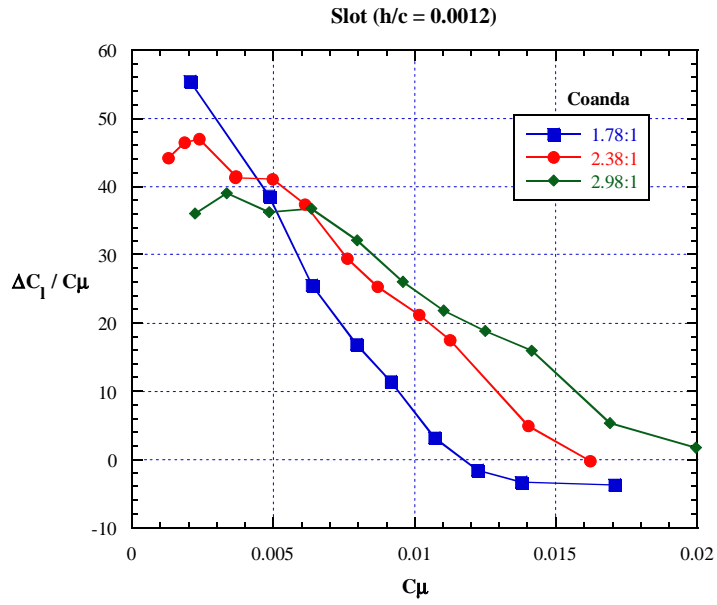
Slot Height

Figure 10 - Lift augmentation, Coanda surface effect, upper slot blowing, Mach = 0.8, $\alpha = +3°$.

417
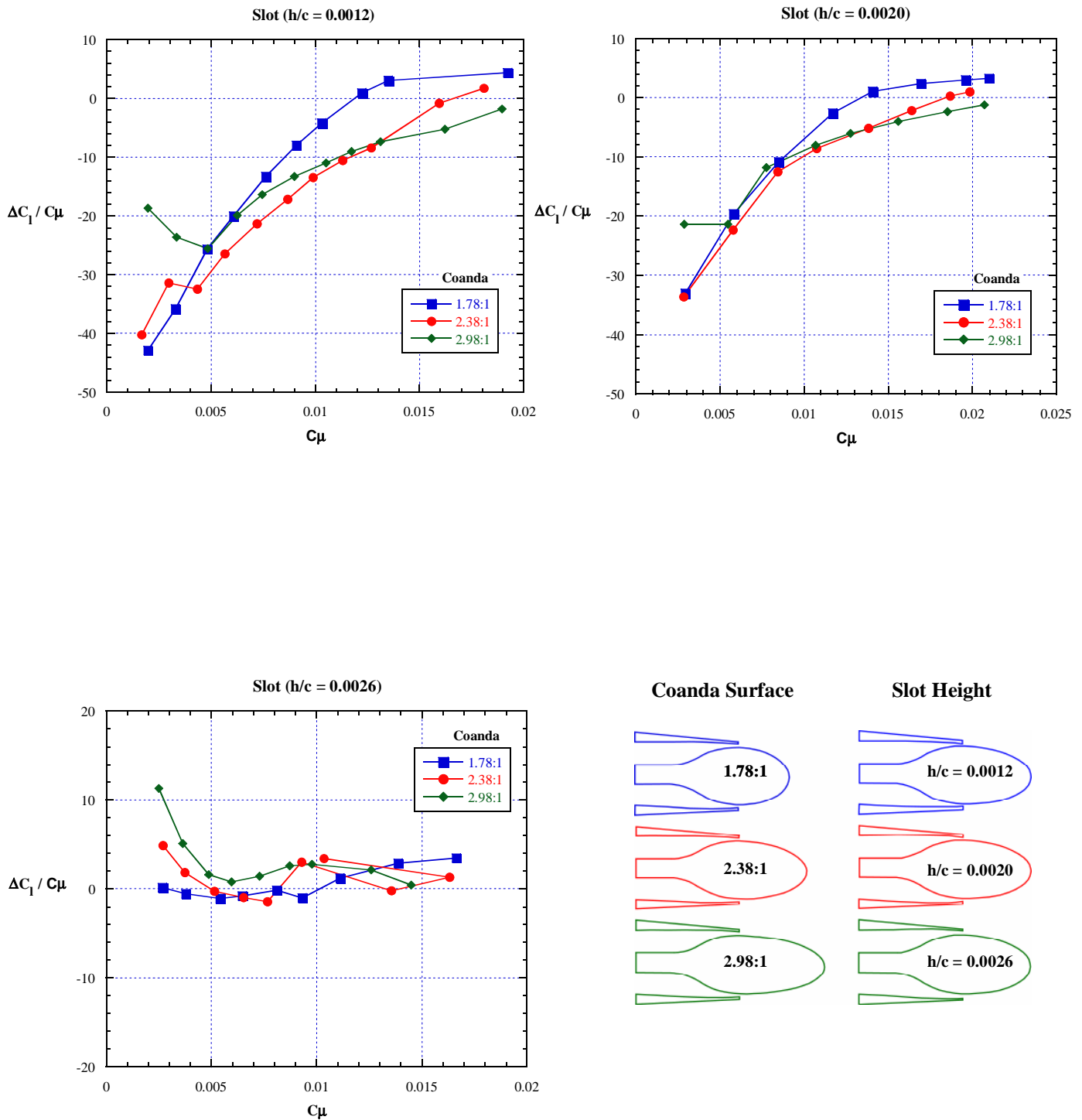
Figure 11 - Lift augmentation, Coanda surface effect, lower slot blowing, Mach = 0.8, α = +3°.
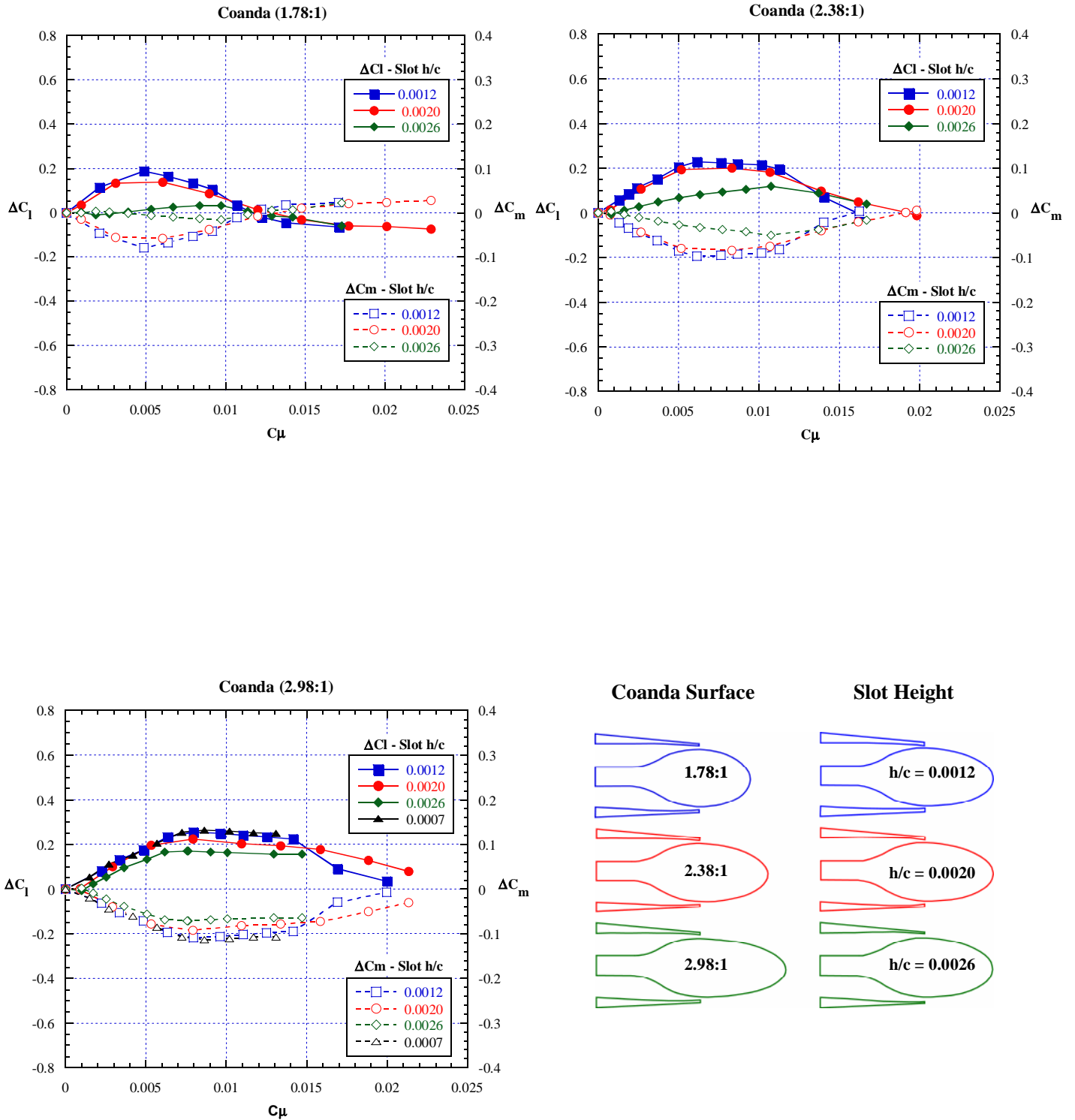
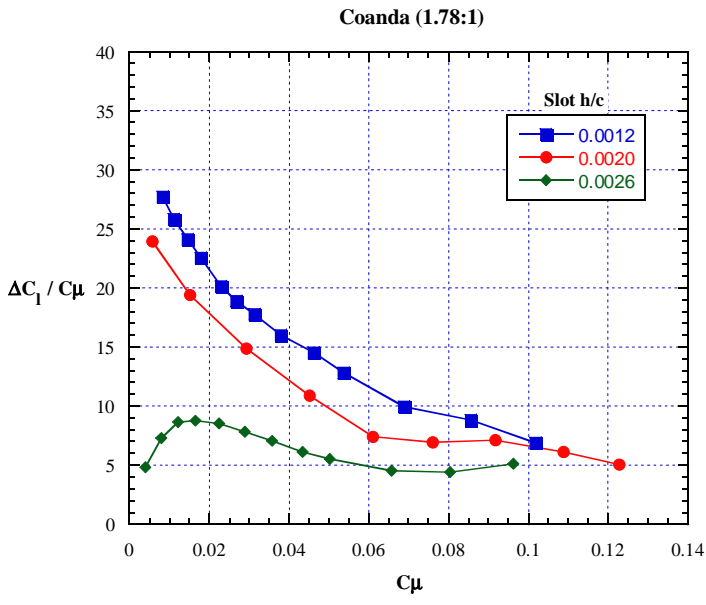Figure 12 - Slot height effect, upper slot blowing, Mach = 0.8, α = +3°.
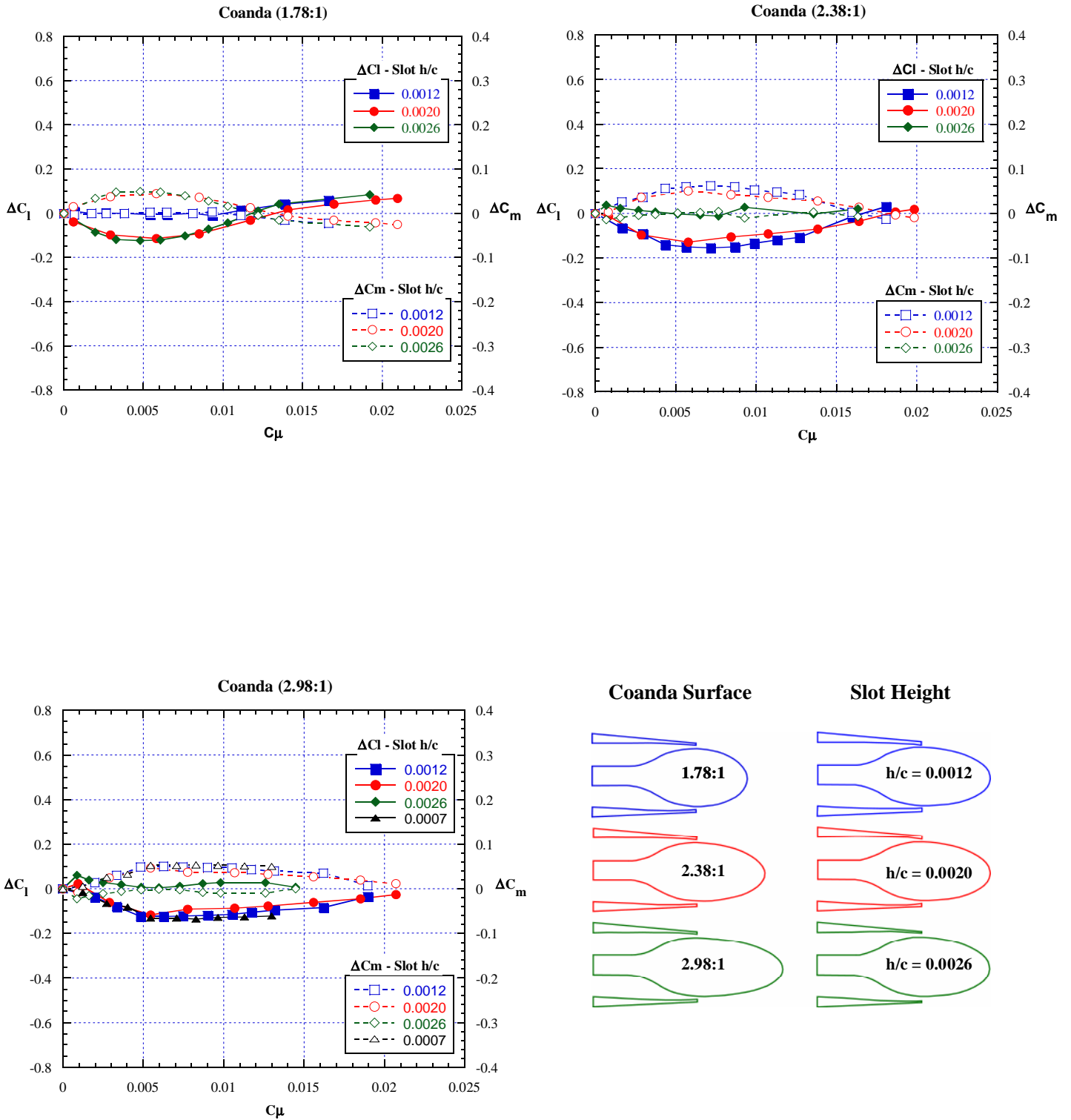
Figure 13 - Slot height effect, lower slot blowing, Mach = 0.8, α = +3°.
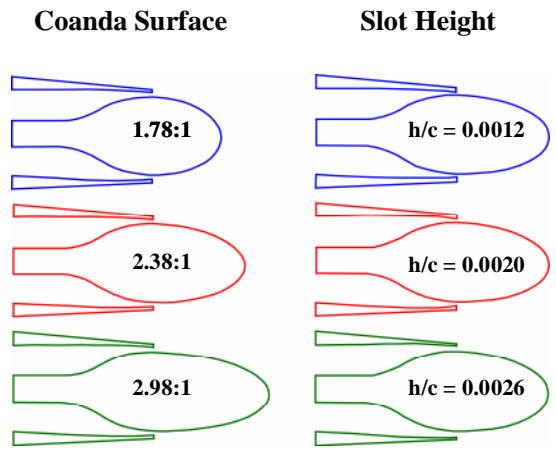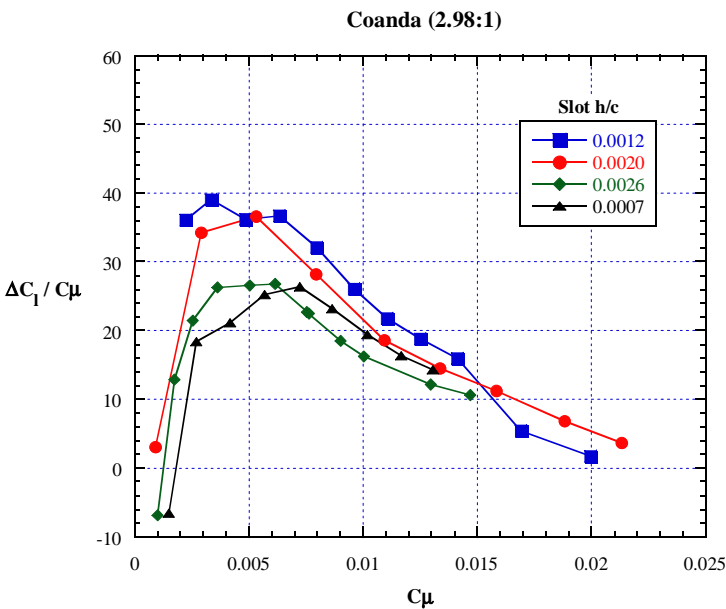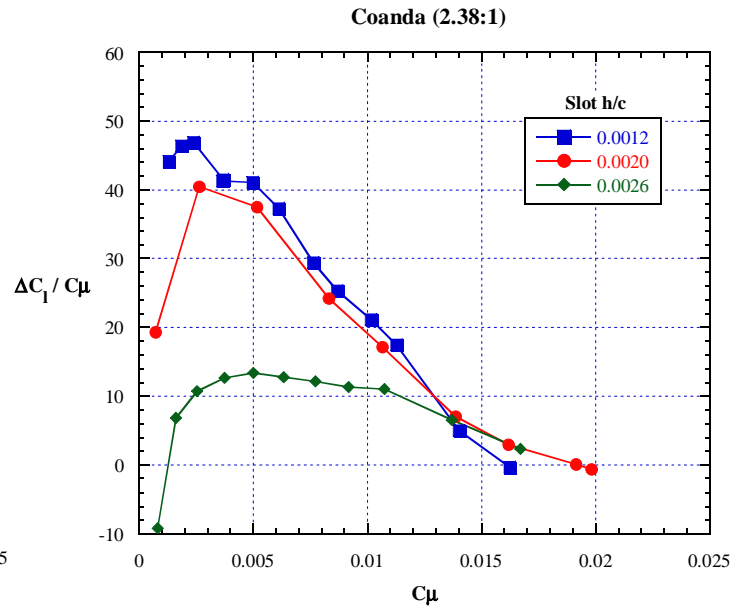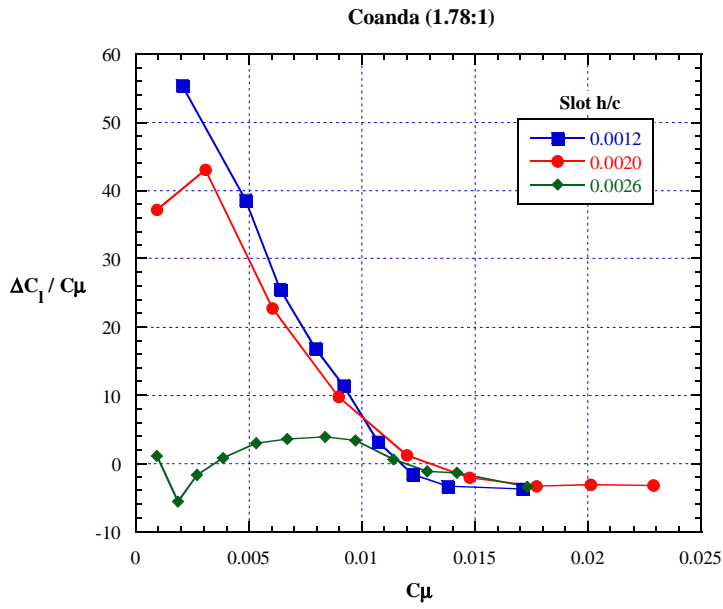
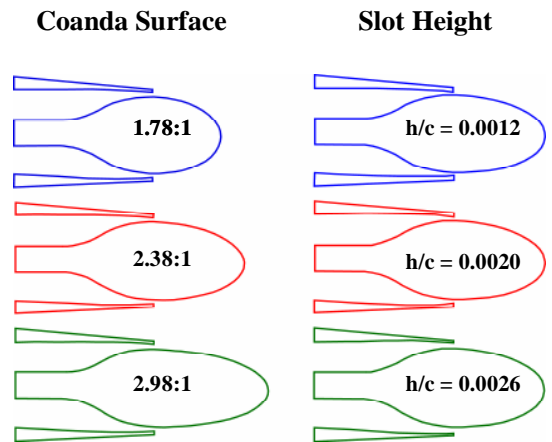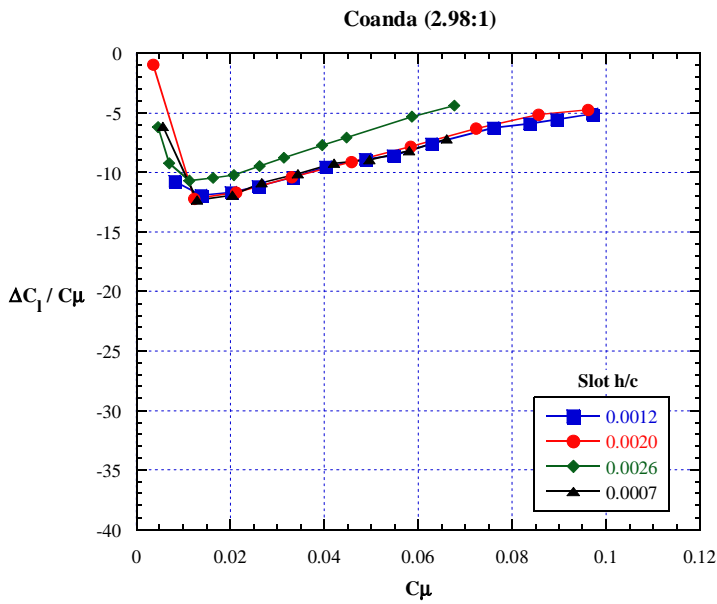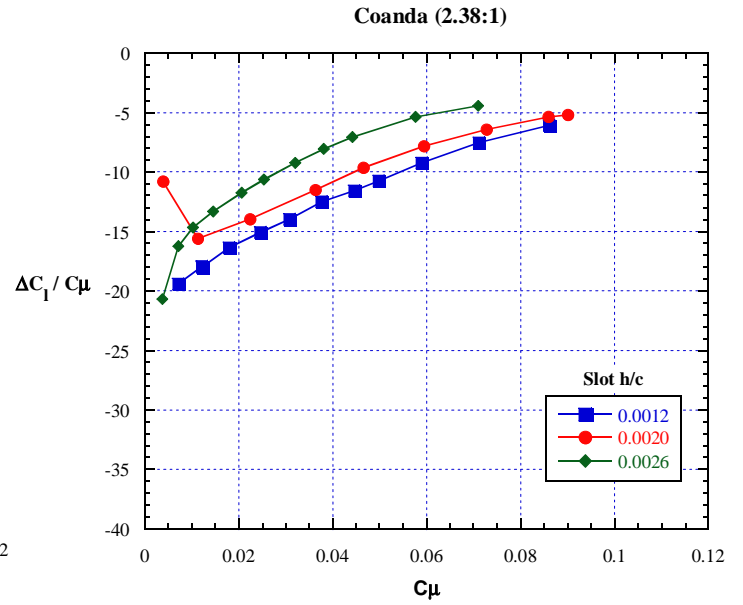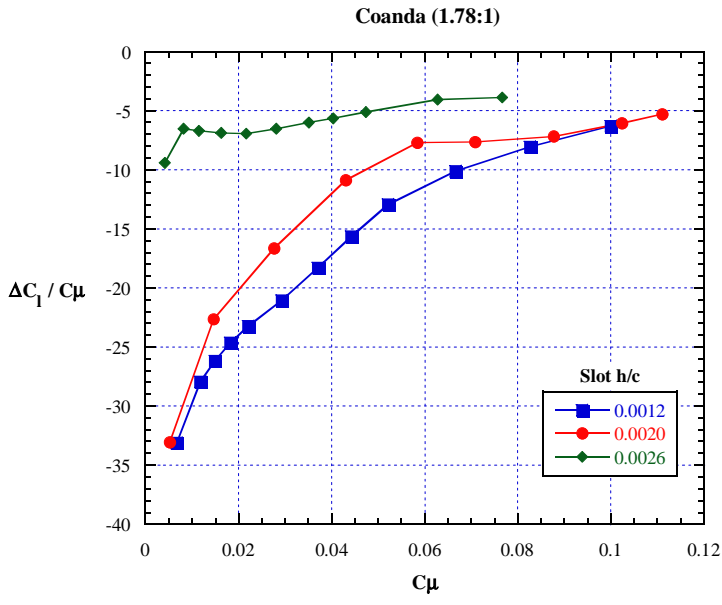Figure 14 - Lift augmentation, slot height effect, upper slot blowing, Mach = 0.8, α = +3°.
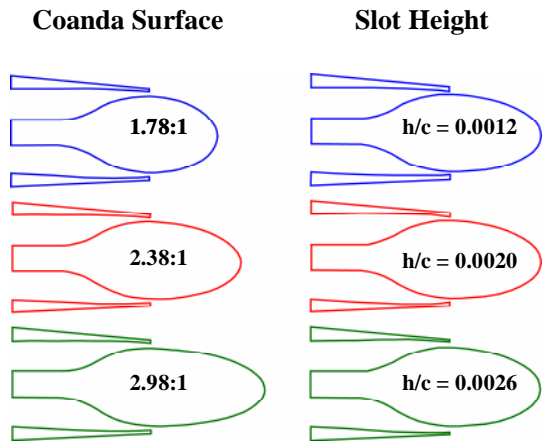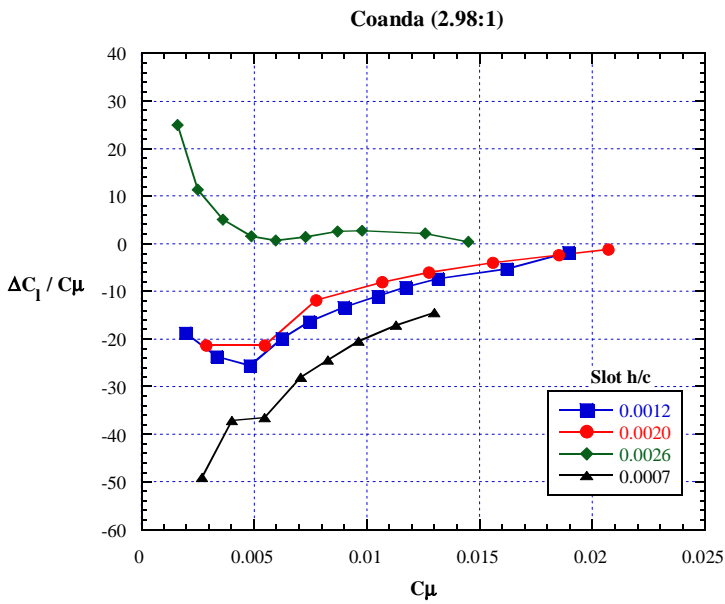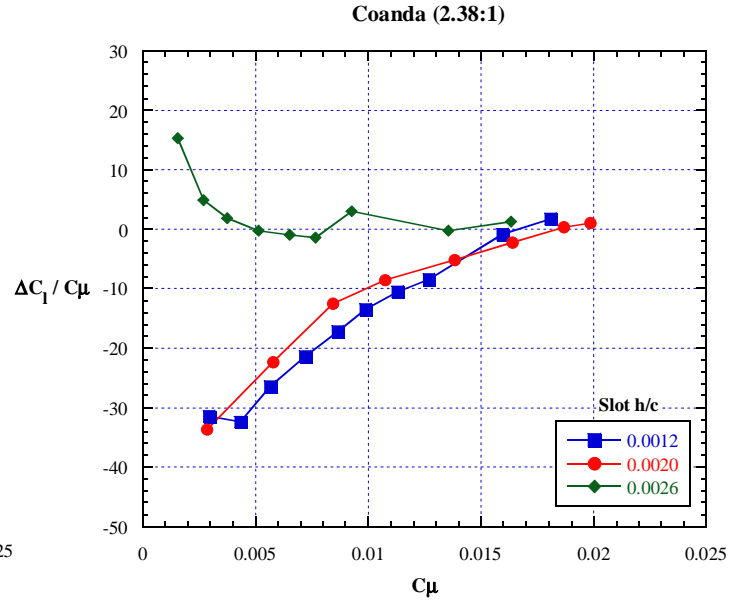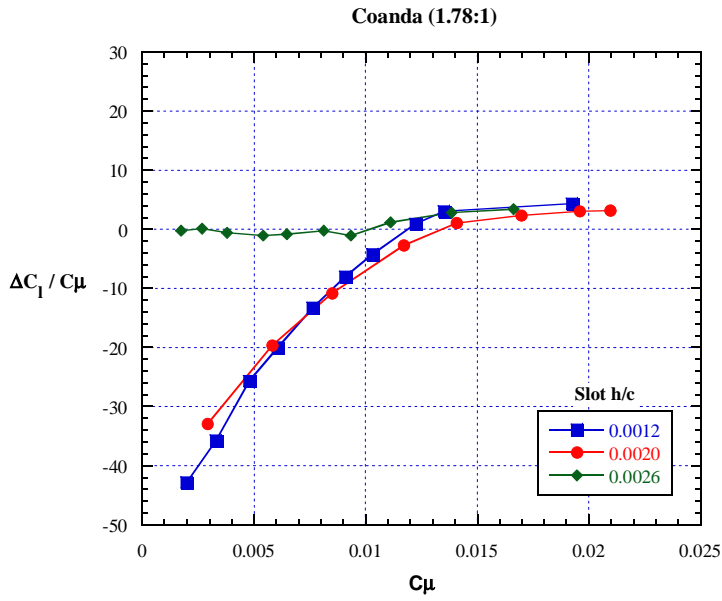
Figure 15 - Lift augmentation, slot height effect, lower slot blowing, Mach = 0.8, $\alpha = +3°$.
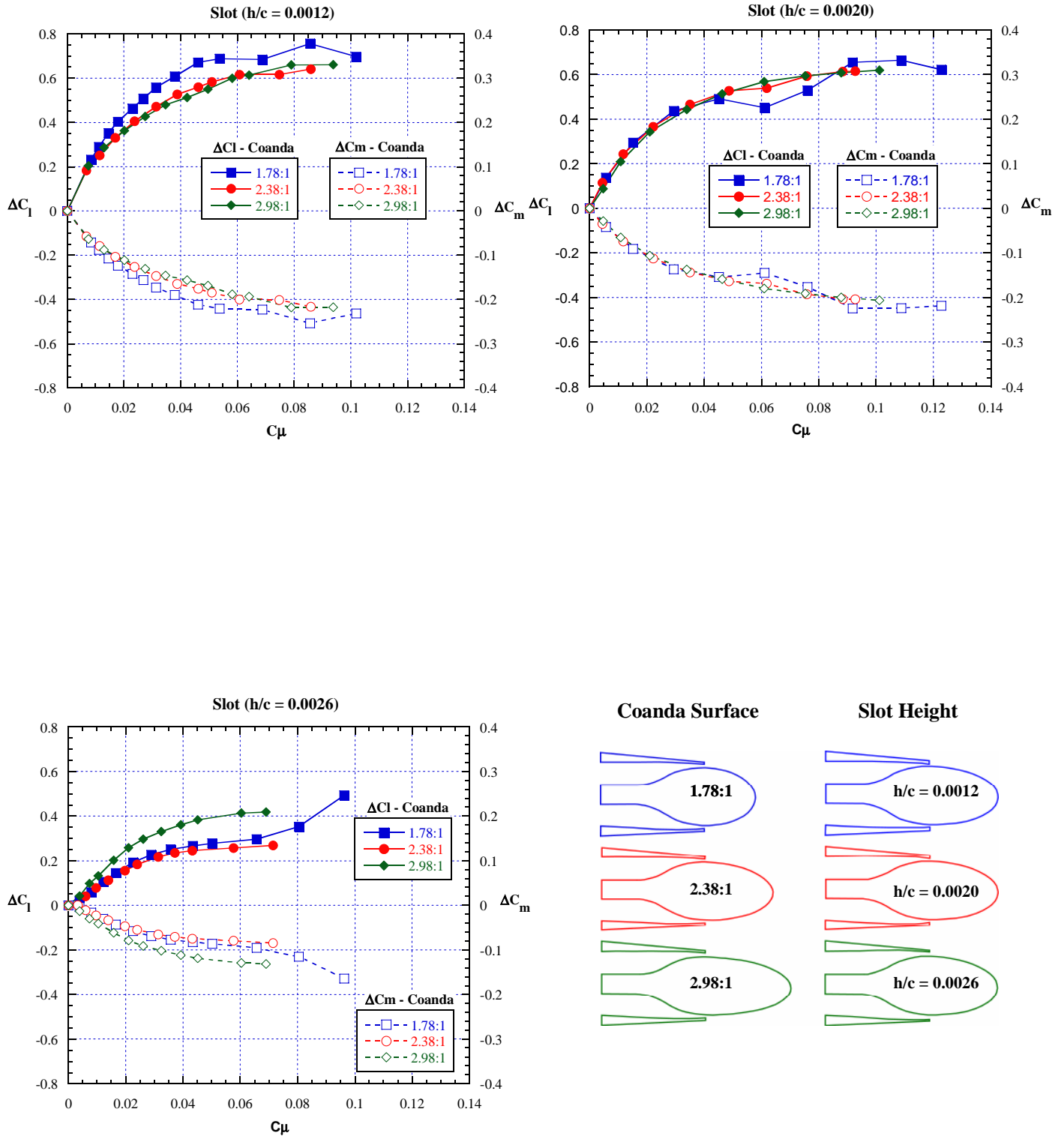
Figure 16 - Coanda surface effect, upper slot blowing, Mach = 0.3, $\alpha = +6°$.
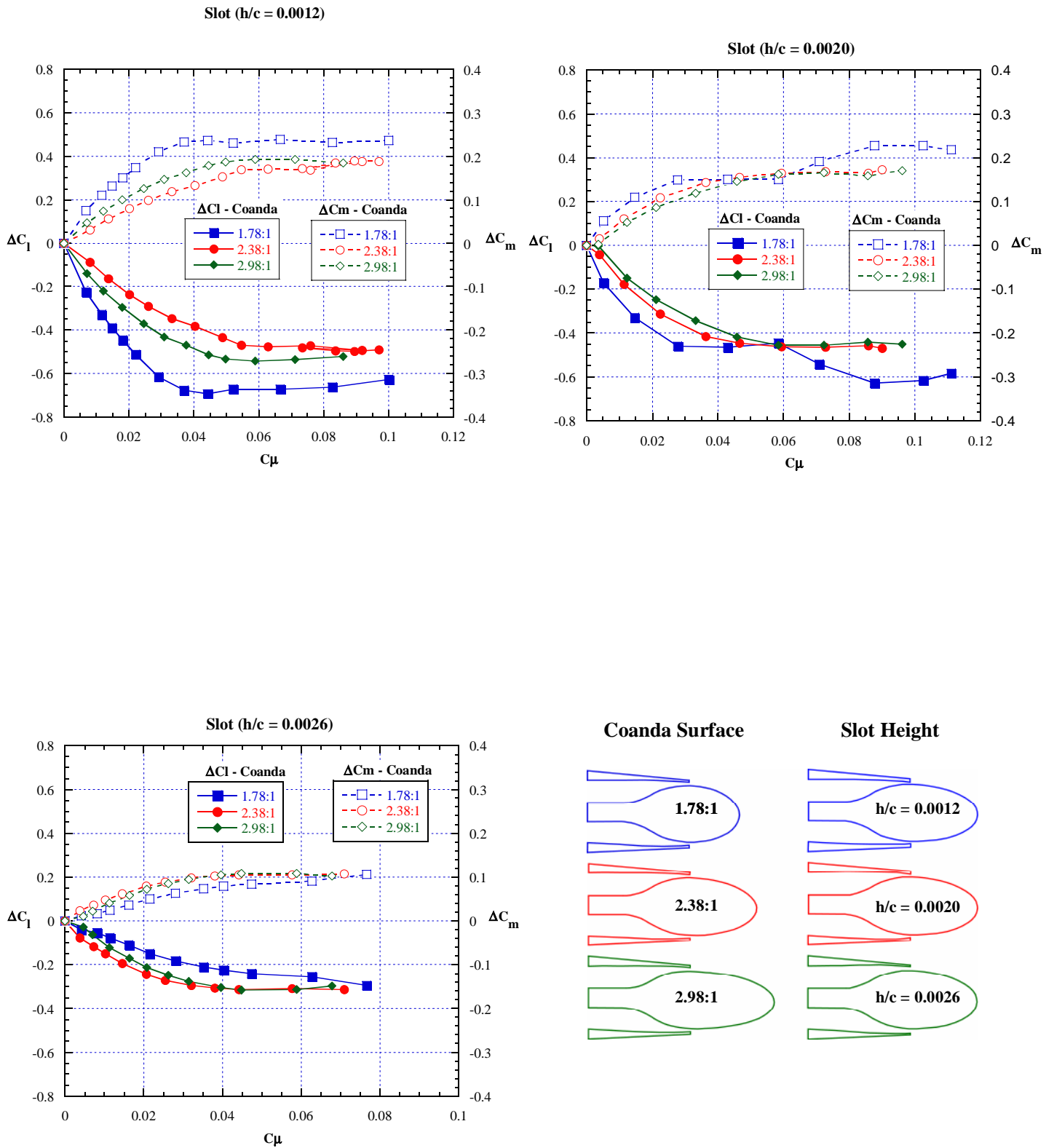
Figure 17 - Coanda surface effect, lower slot blowing, Mach = 0.3, α = +6°.
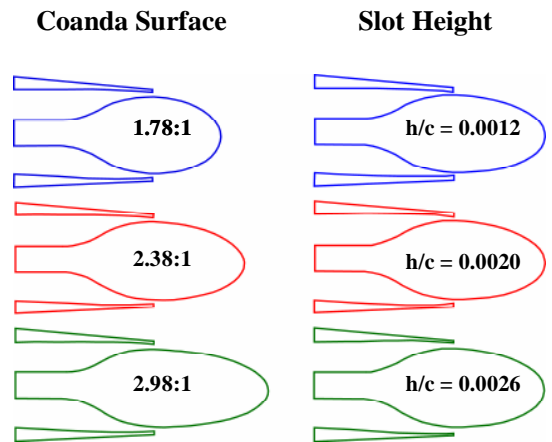
Figure 18 - Lift Augmentation, Coanda surface effect, upper slot blowing, Mach $= 0.3, \alpha = +6°$.
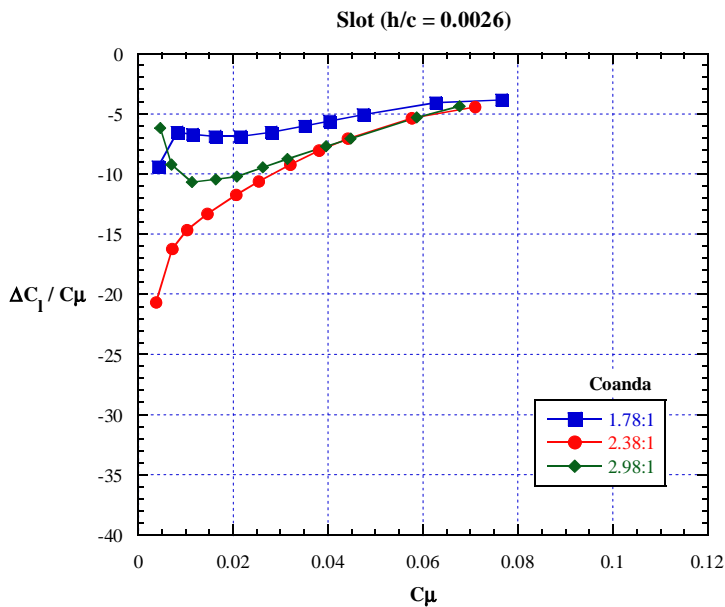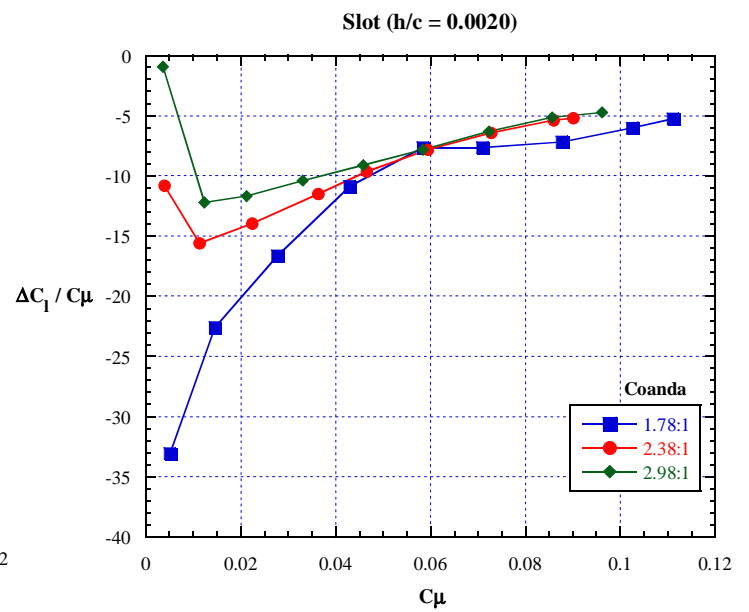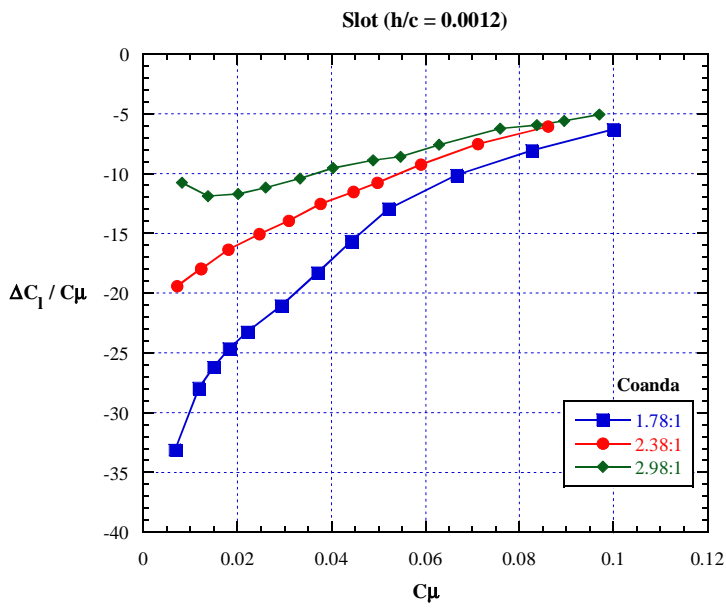
Figure 19 - Lift Augmentation, Coanda surface effect, lower slot blowing, Mach = 0.3, α = +6°.

426
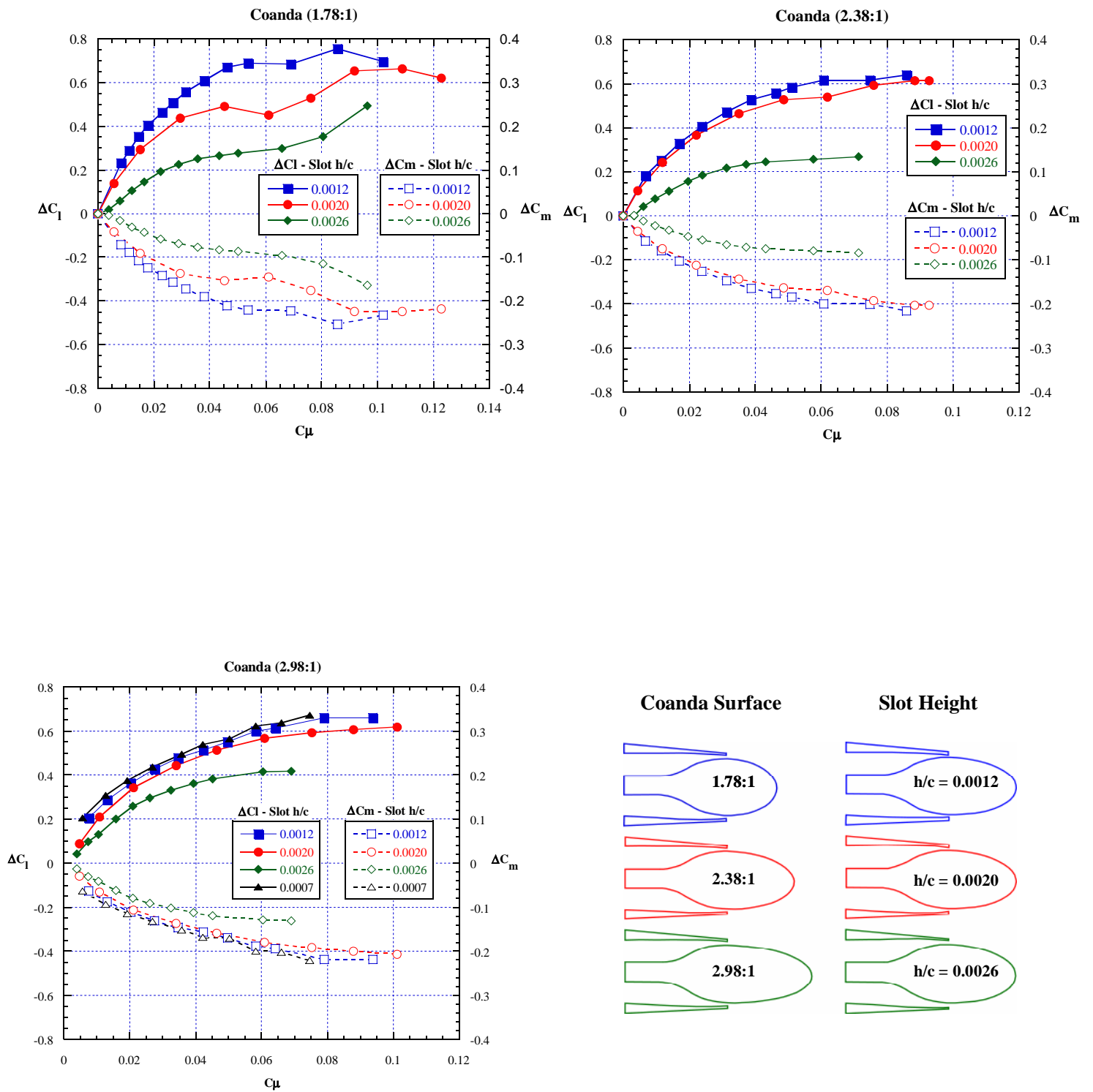
Figure 20 - Slot height effect, upper slot blowing, Mach = 0.3, α = +6°.
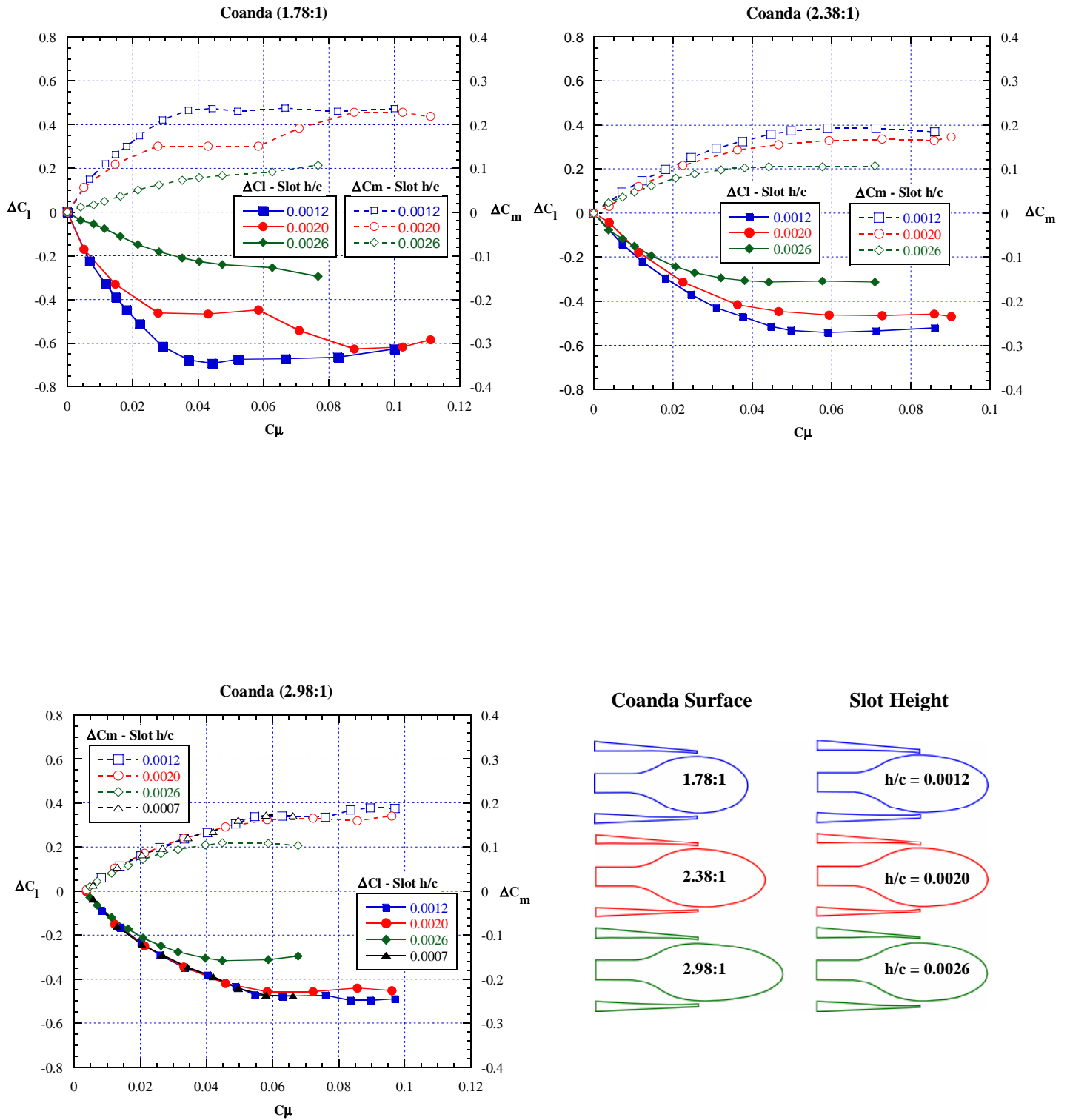
Figure 21 - Slot height effect, lower slot blowing, Mach = 0.3, $\alpha = +6°$.
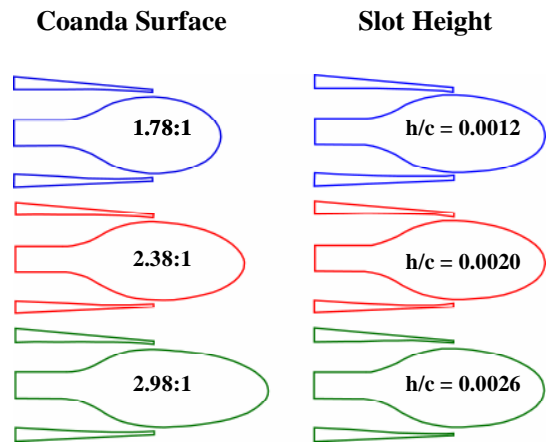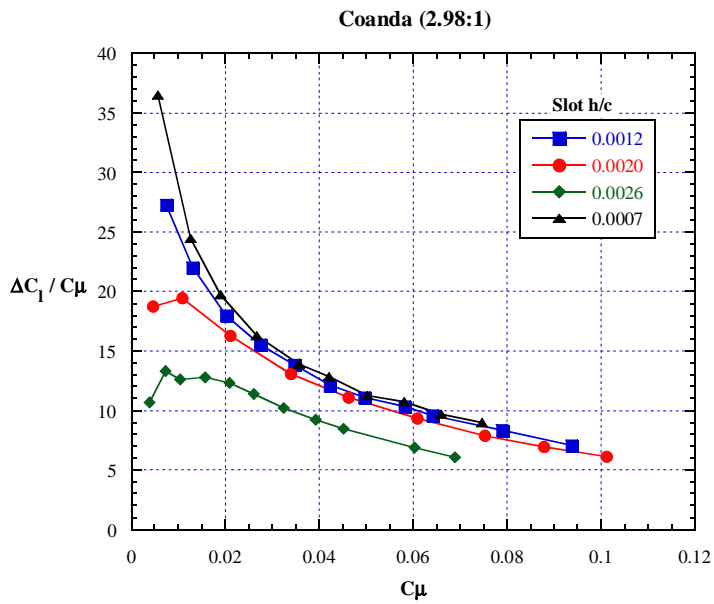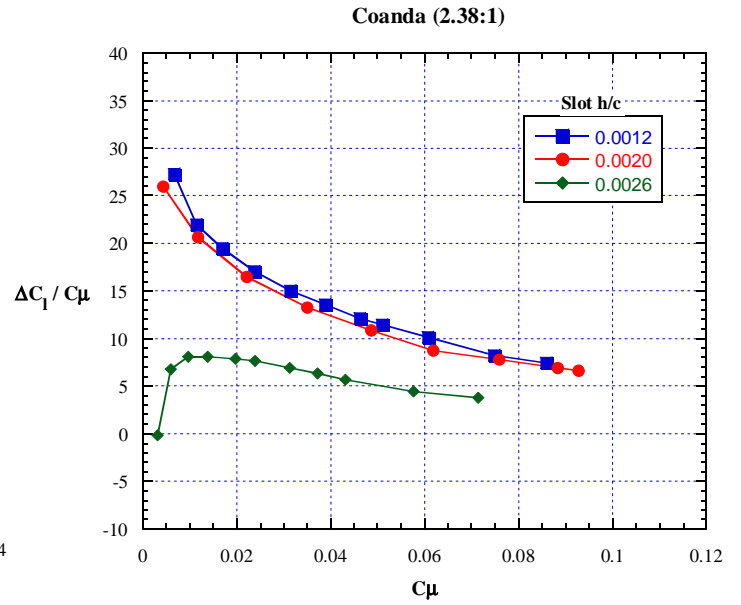
Figure 22 - Lift Augmentation, slot height effect, upper slot blowing, Mach = 0.3, α = +6°.

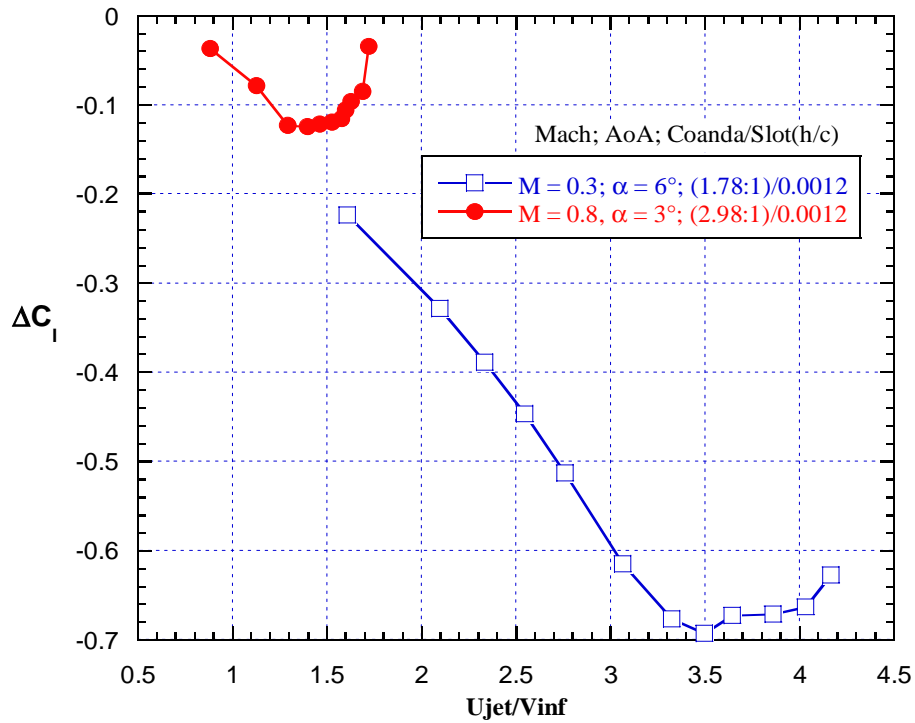Figure 23 - Lift Augmentation, slot height effect, lower slot blowing, Mach = 0.3, $\alpha = +6°$.

Upper surface blowing

Mach; AoA; Coanda/Slot(h/c)
- □ M = 0.3; α = 6°; (1.78:1)/0.0012
- ● M = 0.8, α = 3°; (2.98:1)/0.0012

Lower surface blowing

Mach; AoA; Coanda/Slot(h/c)
- □ M = 0.8; α = 3; (2.98:1)/0.0012
- ● M = 0.3; α = 6; (1.78:1)/0.0012
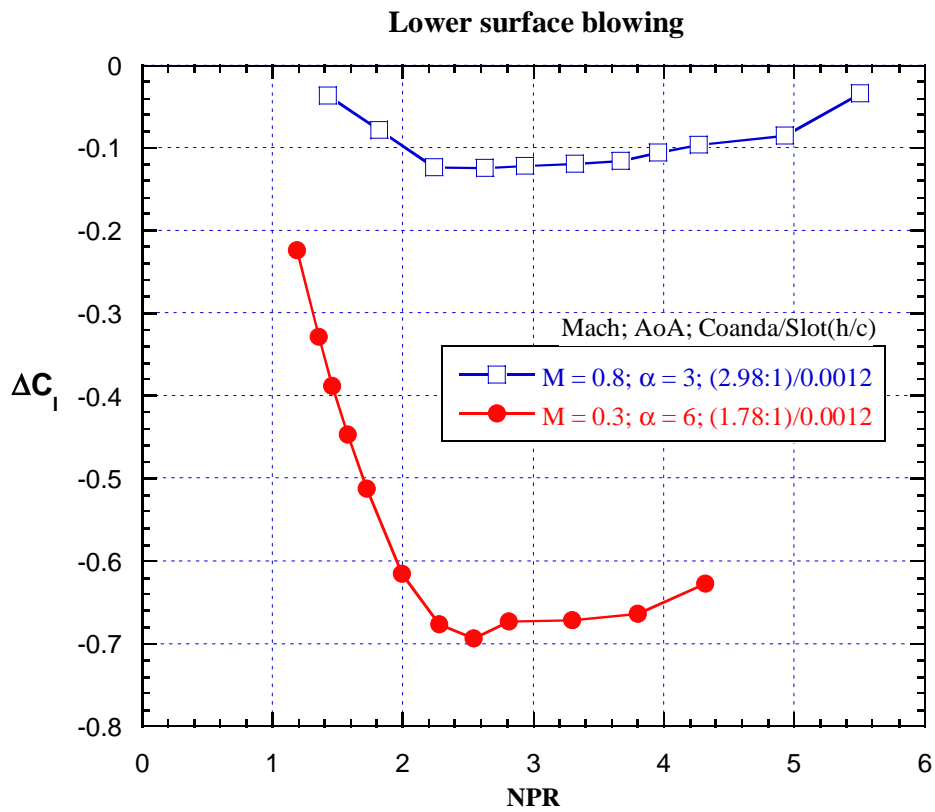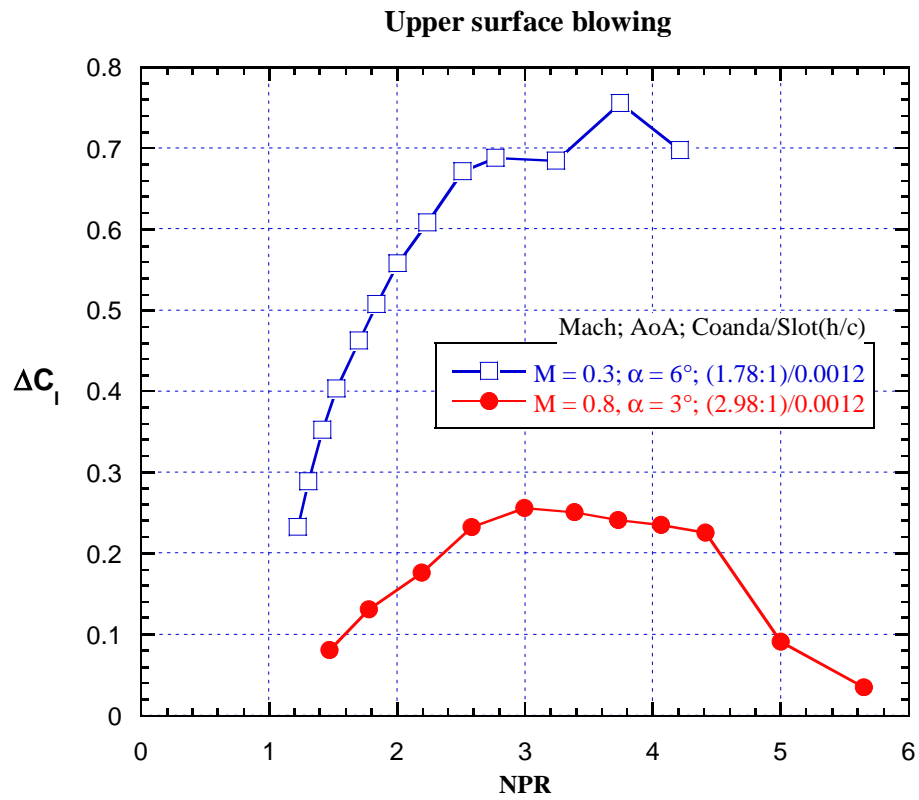
Figure 24 - Nozzle pressure ratio versus ΔC_l, upper and lower slot blowing.

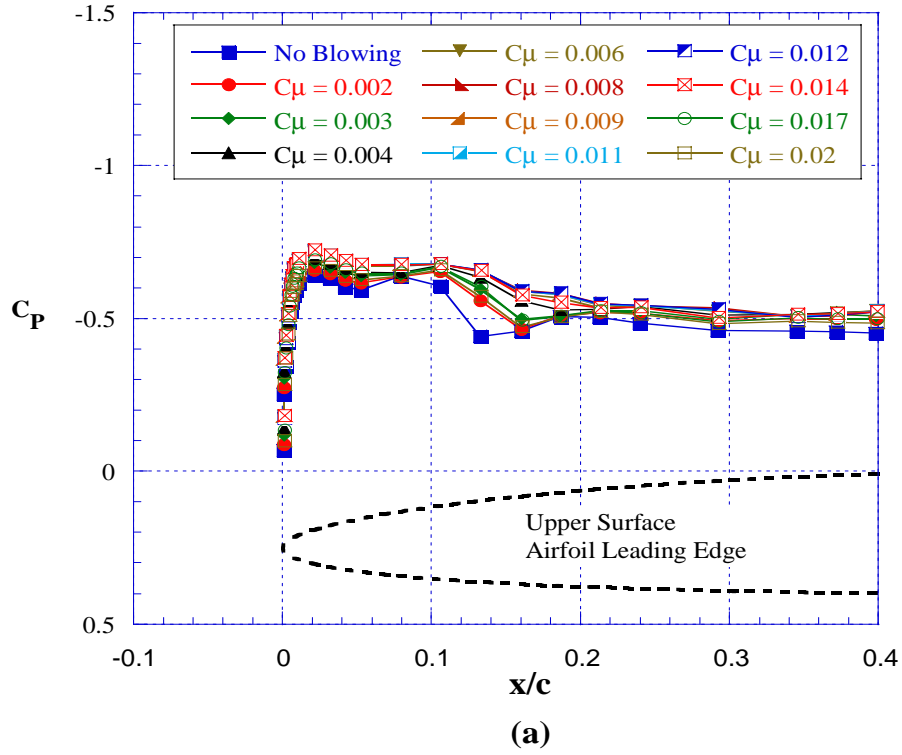**Upper surface blowing**
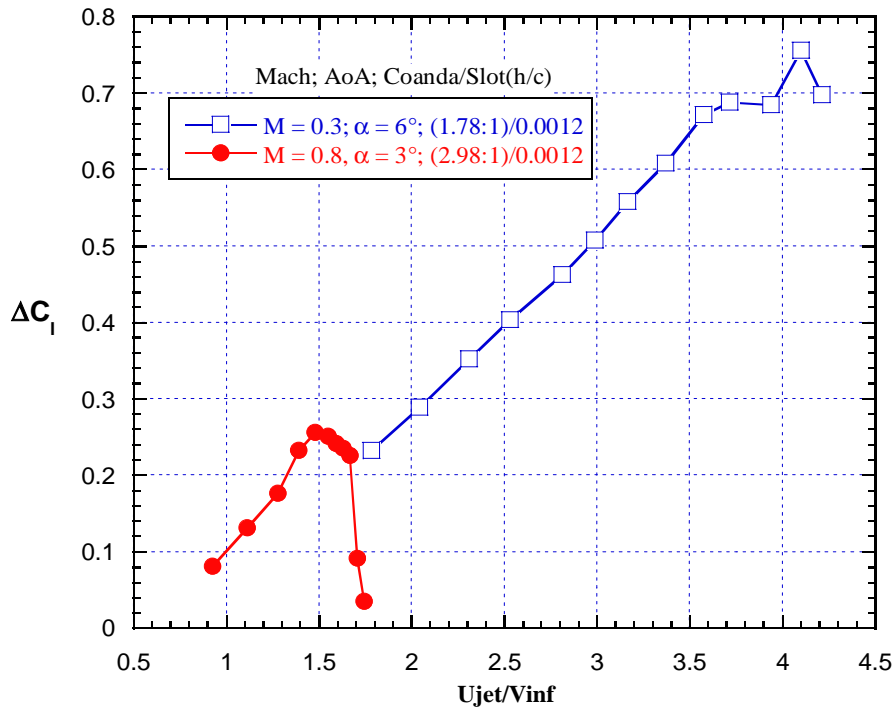
(a)

Lower surface blowing

(b)

Figure 25 - Velocity ratio versus ΔC_l, upper and lower slot blowing.

Upper Surface Leading Edge Pressure Distribution

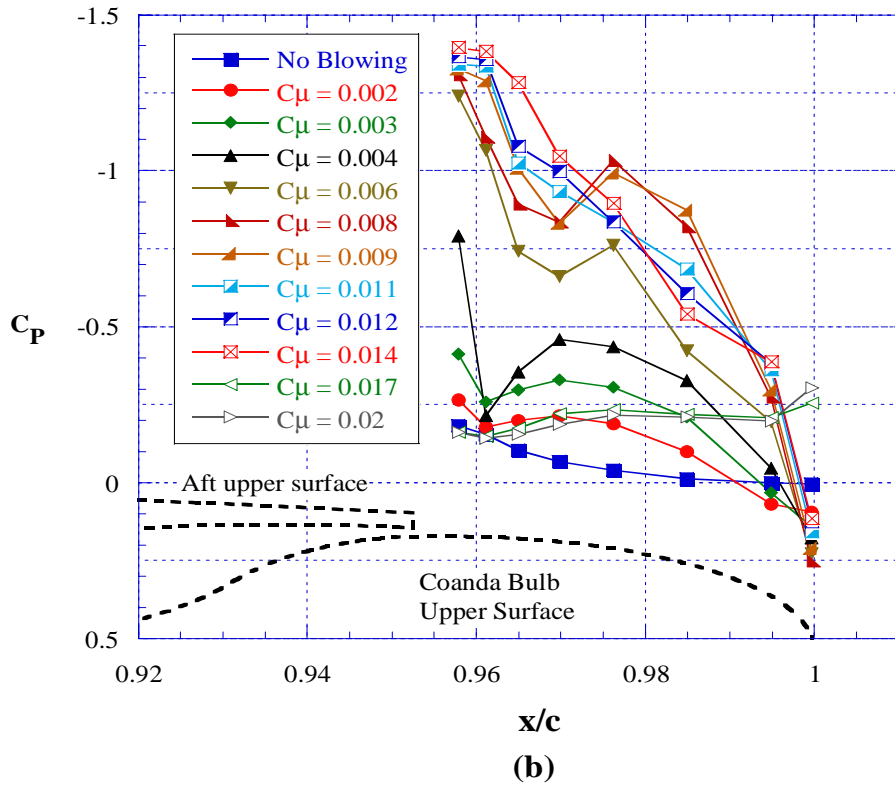**(a)**

Upper Surface Trailing Edge Pressure Distribution

(b)
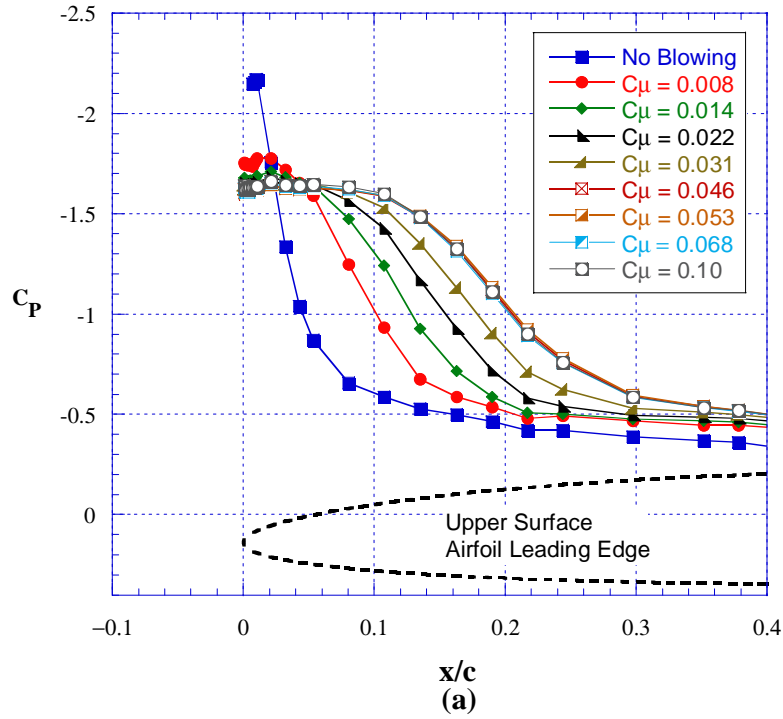
Figure 26 - Pressure distribution, Cμ effect, upper slot blowing;
Coanda (2.98:1), slot (h/c = 0.0012), Mach = 0.8, α = +3°.

Upper Surface Leading Edge Pressure Distribution

(a)

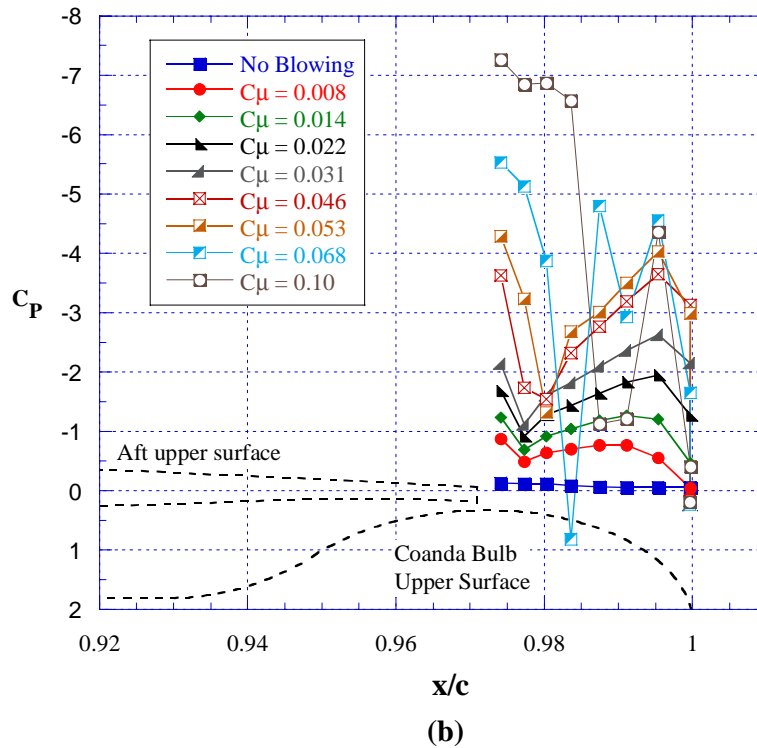**Upper Surface Trailing Edge Pressure Distribution**

(b)

Figure 27 - Pressure distribution, Cμ effect, upper slot blowing;
Coanda (1.78:1), slot (h/c = 0.0012), Mach = 0.3, α = +6°.